



**US Army Corps
of Engineers**
Hydrologic Engineering Center

HEC-RAS USDA-ARS Bank Stability & Toe Erosion Model (BSTEM)

Technical Reference & User's Manual

March 2015

REPORT DOCUMENTATION PAGE				Form Approved OMB No. 0704-0188	
<p>The public reporting burden for this collection of information is estimated to average 1 hour per response, including the time for reviewing instructions, searching existing data sources, gathering and maintaining the data needed, and completing and reviewing the collection of information. Send comments regarding this burden estimate or any other aspect of this collection of information, including suggestions for reducing this burden, to the Department of Defense, Executive Services and Communications Directorate (0704-0188). Respondents should be aware that notwithstanding any other provision of law, no person shall be subject to any penalty for failing to comply with a collection of information if it does not display a currently valid OMB control number.</p> <p>PLEASE DO NOT RETURN YOUR FORM TO THE ABOVE ORGANIZATION.</p>					
1. REPORT DATE (DD-MM-YYYY) February 2015		2. REPORT TYPE Computer Program Documentation		3. DATES COVERED (From - To)	
4. TITLE AND SUBTITLE HEC-RAS USDA-ARS Bank Stability & Toe Erosion Model (BSTEM) Technical Reference & User's Manual				5a. CONTRACT NUMBER	
				5b. GRANT NUMBER	
				5c. PROGRAM ELEMENT NUMBER	
6. AUTHOR(S) CEIWR-HEC				5d. PROJECT NUMBER	
				5e. TASK NUMBER	
				5f. WORK UNIT NUMBER	
7. PERFORMING ORGANIZATION NAME(S) AND ADDRESS(ES) US Army Corps of Engineers Institute for Water Resources Hydrologic Engineering Center (HEC) 609 Second Street Davis, CA 95616-4687				8. PERFORMING ORGANIZATION REPORT NUMBER CPD-68B	
9. SPONSORING/MONITORING AGENCY NAME(S) AND ADDRESS(ES)				10. SPONSOR/ MONITOR'S ACRONYM(S)	
				11. SPONSOR/ MONITOR'S REPORT NUMBER(S)	
12. DISTRIBUTION / AVAILABILITY STATEMENT Approved for public release; distribution is unlimited.					
13. SUPPLEMENTARY NOTES					
14. ABSTRACT The HEC-RAS (Hydrologic Engineering Center's (HEC) River Analysis System) software has included mobile bed capabilities since Version 4.0. These capabilities compute vertical bed changes in response to dynamic sediment mass balance and bed processes. However, many riverine sediment problems involve lateral bank erosion that does not fit in the current computational paradigm. The Bank Stability and Toe Erosion Model (BSTEM) developed by the National Sediment Laboratory, United States Department of Agriculture (USDA), Agricultural Research Station (ARS) is a physically based model that accounts for the dominant stream bank processes but requires an intermediate level of complexity and parameterization. This method was selected for implementation in HEC-RAS.					
15. SUBJECT TERMS HEC-RAS, BSTEM, USDA-ARS, Bank Stability & Toe Erosion Model, bank failure, soil forces, failure block, hydrostatic, pore water pressure,					
16. SECURITY CLASSIFICATION OF:			17. LIMITATION OF ABSTRACT UU	18. NUMBER OF PAGES 74	19a. NAME OF RESPONSIBLE PERSON
a. REPORT U	b. ABSTRACT U	c. THIS PAGE U			19b. TELEPHONE NUMBER

HEC-RAS

USDA-ARS Bank Stability & Toe Erosion Model (BSTEM)

DRAFT

Technical Reference & User Manual

February 2015

US Army Corps of Engineers
Institute for Water Resources
Hydrologic Engineering Center
609 Second Street
Davis, CA 95616

(530) 756-1104
(530) 756-8250 FAX
www.hec.usace.army.mil

CPD-68B

Table of Contents

List of Figures	iii
List of Tables	v
Background.....	vii

Technical Reference Manual

Chapter	Page No.
TR.1 Bank Failure	TR-1
TR.1.1 Layer Method	TR-2
TR.1.1.1 Soil Forces.....	TR-4
Weight of the Soil in the Failure Block.....	TR-4
Cohesion	TR-4
TR.1.1.2 Hydraulic Forces.....	TR-4
Hydrostatic Confining.....	TR-5
Pore Water Pressure	TR-5
TR.1.2 Method of Slices	TR-7
TR.1.2.1 Tension Cracks.....	TR-11
TR.1.2.2 Cantilever Failures.....	TR-12
TR.1.3 Selecting a Method	TR-13
TR.1.4 Steps in a Bank Failure Analysis.....	TR-14
TR.2 Toe Erosion (Fluvial or Hydraulic Erosion) - Flow Driven.....	TR-19
TR.2.1 Determining the Zone of Scour	TR-19
TR.2.2 Determining τ_{node}	TR-19
TR.2.3 Scour	TR-22

User's Manual

Chapter	Page No.
UM.1 Getting Started	UM-1
UM.2 Defining Cross Section Configuration	UM-2
UM.3 Defining Cross Section Materials.....	UM-4
UM.4 USDA-ARS BSTEM Options	UM-13
UM.4.1 Number of Failure Plane Computation Nodes	UM-14
UM.4.2 Number of Time Steps between Failure Computations	UM-14
UM.4.3 Grain Shear Correction	UM-14
UM.4.4 Minimum Percent Cohesive to Use Toe Scour Algorithms	UM-14
UM.4.5 Transport Function.....	UM-15
UM.4.6 Toe Scour Mixing Method	UM-16
UM.5 Output	UM-17
UM.6 Model Validation.....	UM-17
UM.7 Modeling Guidelines, Tips, and Troubleshooting	UM-20
UM.7.1 Stepwise Modeling Process	UM-20
UM.7.2 Selecting a Toe.....	UM-23

Table of Contents

User's Manual (continued)

Chapter	Page No.
UM.7.3 Monotonic Bank Geometry	UM-24
UM.7.4 Floodplain Geometry	UM-24
UM.7.5 Too Much Scour	UM-25
UM.7.6 Common Runtime Error Messages	UM-25
UM.7.7 Unusual Cross Section Shape	UM-27
UM.7.8 Groundwater Table	UM-27
UM.7.9 Scour Outside of a Bend	UM-28
UM.8 Acknowledgements	UM-28
UM.9 Scour Units	UM-29
UM.10 SI Table	UM-30
UM.11 References	UM-30

List of Figures

Figure Number	Page No.
1 Force diagram for the "Layer Method" from Simon, 2000	TR-2
2 Components of the hydrostatic forces acting normal to and along the failure plane	TR-5
3 Idealized hydrostatic assumption of positive and negative pore water pressure with respect to the groundwater surface and potential empirical divergence from the assumption	TR-6
4 Relationship between measured or computed matrix suction and the empirical strength "apparent cohesion" defined by the ϕ^b parameter	TR-7
5 Subdivision of layers into slices. The failure block through each layer is divided into three slices of equivalent width	TR-7
6 Forces acting on a slice	TR-8
7 Schematic of how the ratio of inter-slice shear stress to inter-slice normal stress ($\lambda=0.4$) is reduced by $f(x)$ depending on the proximity of the slice to the center of the failure block	TR-9
8 Iterative scheme to compute FS for the method of slices including the dependency of the Normal Force at the base of the slice on the inter-slice forces.	TR-10
9 Tension crack computation criteria	TR-11
10 A taxonomy of cantilever failure mechanisms (after Thorne and Tovoy, 1981)	TR-12
11 Example of maximum failure plane angles for overhanging bank situations where β_{max} is greater than or equal to ninety degrees. These classify as cantilever failures and the software will force a method of slices analysis.....	TR-13
12 Theoretical difference in normal stress computed by Layer Method and Method of Slices.....	TR-14
13 Multiple failure planes have to be evaluated at multiple nodes	TR-14
14 Computing the maximum and minimum failure angles and first guess.....	TR-16
15 Factor of Safety computed for the maximum and minimum angles and the initial estimate.....	TR-16
16 A parabolic function is fit to the three points and a) function minimum is selected as the next failure plane and b) computes a FS associated with that failure plane and the residual between the FSs predicted by the method.....	TR-17
17 The new FS computed for β_i becomes the new maximum or minimum and a tighter polynomial is fit to the new three points to identify a new function minimum.....	TR-18
18 Monotonic β - FS function associated with a cantilever failure	TR-18
19 Subdividing the cross section into vertical conveyance prisms (blue) versus zones (yellow) perpendicular to the isovels (green)	TR-20
20 Finding the bisecting angle at the toe which will determine the portion of the water column that is contributing to toe scour.....	TR-20
21 The orientation of the radial prisms used to compute a shear at each node is computed by proportioning the intersection of the water surface with the depth within the scour zone.....	TR-21

List of Figures

Figure Number	Page No.
22 Apportioning the local shear by a ratio of the hydraulic radius of the radial prisms.....	TR-21
23 Nodes between the movable bed limits are adjusted vertically (and uniformly) and the wetted nodes outside the movable bed limits are adjusted laterally (and independently).....	TR-22
24 Overhanging bank simplification method	TR-22
25 HEC-RAS Main Window	UM-1
26 HEC-RAS - Sediment Data Editor - USDA-ARS BSTEM Tab	UM-1
27 Definition of stations points for BSTEM half cross sections.....	UM-2
28 Reasonable location for Edge of Bank and Top of Toe definitions on an HEC-RAS cross section	UM-3
29 (a) The maximum, minimum and incremental angles evaluated (b) at each node between the Top of Toe and Edge of Bank	UM-3
30 Idealized gradations selected for the default material types.....	UM-6
31 HEC-RAS - Sediment Data Editor - BSTEM Tab - Selecting Cross Section Materials.....	UM-6
32 BSTEM Material Parameters Editor	UM-7
33 ϕ^b is the slope of the relationship between matrix suction and apparent cohesion	UM-9
34 Defining bed gradations.....	UM-9
35 Relationship between erodibility and critical shear stress from Simon, 2000	UM-10
36 Groundwater response to (a) high (b) low and (c) moderate hydraulic conductivities.....	UM-11
37 Selecting the layer mode for a bank failure.....	UM-12
38 Defining layers and layer material types	UM-12
39 Guidelines for setting layer elevations	UM-13
40 BSTEM Options Editor	UM-13
41 BSTEM Options Editor - Transport functions available for cohesionless toe scour in BSTEM	UM-15
42 Time series of bank mass eroded by process.....	UM-17
43 Time series of FS	UM-18
44 Groundwater and water surface time series plot demonstrating the lag between water surface and groundwater elevations	UM-18
45 Requesting and specifying the frequency of sediment cross section output in the Sediment Output Options dialog box	UM-19
46 Example HEC-RAS cross section output including toe scour, incision and bank failure at various stages in the simulations	UM-20
47 Bank migration cross section output with the new Sediment Output viewer	UM-21
48 Output from a validation test of the HEC-RAS implementation of the bank failure capabilities and the standalone models	UM-21

List of Figures

Figure Number	Page No.
49 Select Goodwin Creek repeated right bank surveys at the two central cross sections with HEC-RAS/BSTEM cross section migration from Gibson, 2015.....	UM-22
50 Cross section view adjusted to approximately to 1:1 aspect ratio to help select the toe station.....	UM-23
51 Avoid bank depressions (left) where possible, particularly with soil layers. Monotonic banks (cross section nodes that increase from the toe out to the bank edge) are more stable	UM-24
52 BSTEM requires cross section station-elevation points between the Bank Edge Station and the end of the cross section	UM-25
53 In this model, the cohesionless transport methods computed more than 100 feet of bank scour in just a month, which is order of magnitude faster than the actual bank recession rate	UM-25
54 The Unrealistic Vertical Adjustment Error	UM-26
55 Strange cross section shape caused by deposition inside the movable bed limits, but no outside.....	UM-27
56 The same simulation as in Figure 55, but allowing for deposition in the overbanks.....	UM-27

List of Tables

Table Number	Page No.
1 Method selection criteria.....	TR-13
2 Default materials and material parameters	UM-5
3 USDA-ARS BSTEM Output Variables in HEC-RAS	UM-19
4 Conversion Factors	UM-29
5 Default materials and material parameters	UM-29

Background

The HEC-RAS (Hydrologic Engineering Center's (HEC) River Analysis System) software has included mobile bed capabilities since Version 4.0. These capabilities compute vertical bed changes in response to dynamic sediment mass balance and bed processes. However, many riverine sediment problems involve lateral bank erosion that does not fit in the current computational paradigm. There are a number of published methodologies for computing bank failure. The methodologies span a spectrum from basic angle of repose methods that require very few parameters but simplify bank processes considerably, to comprehensive geotechnical bank stability models that require a full suite of geotechnical parameters yet lack a framework for hydraulic toe feedbacks. The Bank Stability and Toe Erosion Model (BSTEM) developed by the National Sediment Laboratory, United States Department of Agriculture (USDA), Agricultural Research Station (ARS) is a physically based model that accounts for the dominant stream bank processes but requires an intermediate level of complexity and parameterization. This method was selected for implementation in HEC-RAS.

BSTEM (Simon, 2000; Langendoen, 2008; Simon, 2010) couples iterative, planer bank failure analysis based on a fundamental force balance, with a toe scour model that allows feedback between the hydraulic dynamics on the bank toe which could exacerbate failure risk (in the case of toe scour) or decrease failure risk (in the case of toe protection). The goal of coupling HEC-RAS with BSTEM is to build a model that simulates feedbacks between bed and bank processes. For example, if HEC-RAS computes a decrease in the regional base level or local channel scour it will decrease bank stability and increase the risk of a failure. Similarly, when a bank does fail, the bank material will be added to the sediment mass balance of the mobile bed model which will simulate the river's capacity to "metabolize" and transport these point sources.

USDA-ARS Bank Stability and Toe Erosion Model (BSTEM) in HEC-RAS

Technical Reference Manual

As the name suggests, BSTEM includes two major, interacting components, a bank failure model and toe scour algorithms:

1. **Bank Failure:** A geotechnical bank failure model computes failure planes through the bank to determine if the gravitational driving forces exceed the frictional resisting forces (and the interactions of pore water pressure).
2. **Toe Scour:** An erosion model simulates lateral bank migration, hydraulic forces that undercut the bank. As the toe scours, the bank becomes less stable, so toe scour can initiate bank failure.

These two processes also interact with a third process native to the classic sediment methodology in HEC-RAS computations:

3. **Vertical Erosion or Deposition:** The vertical adjustment of the cross section can also decrease the stability of the bank and interact with toe scour computations. Conversely, a large bank failure could add enough sediment mass to the system to deposit downstream and increase the stability of downstream banks.

Modeling the interactions and feedbacks between these three processes were the main motivation for including the USDA-ARS BSTEM algorithms into HEC-RAS. The science, methods and math of vertical erosion and deposition are covered in the HEC-RAS User's Manual (HEC, 2016a) and the HEC-RAS Hydraulic Reference Manual (HEC, 2016b).

TR.1 Bank Failure

The bank failure methods employ classical, planar, analyses to compare gravitational driving forces of the soil, soil water and overburden, and frictional resisting forces (including the influences of pore water pressure) to determine the most likely failure plane through the bank and to compute whether that failure plane is stable. If the weakest failure plane is unstable, the bank fails and the sediment from the failed bank is added to the sediment transport model.

The bank stability model goes through a series of iterative computations to select potential failure planes, evaluate the factor of safety, and converge on the failure plane most likely to fail by following the following steps:

1. Find the Factor of Safety (FS) for nodes at several vertical locations on the bank.
2. Select the bounding Failure Planes (minimum and maximum angles) and compute a critical factor of safety (FS_{cr}) for each vertical location (in Step 1).

3. Select a most probable critical failure plane ($FS_i \sim FS_{cr}$)
4. Compute the FS_i
5. Use that information to update the critical failure plane ($FS_{i+1} \rightarrow FS_{cr}$) using the "bracket and Brent" optimization algorithm (Teukolsky, 2007)
6. Decide when the FS is close enough to FS_{cr} to stop
7. If FS_{cr} is less than one, fail the bank, update the cross section, and transfer the bank sediments to the routing model

The failure plane selection and optimization algorithms are covered Sections TR.1.1 and TR1.1.2. Since most of the physical algorithms are embedded in the FS computation for each failure plane (Step 3), the description starts with these basic physics and then moves to the optimization scheme.

BSTEM includes two computational approaches to computing the FS of a failure plane through the bank:

- i. Layer Method
- ii. Method of Slices

TR.1.1 Layer Method

The Layer Method is based on Simon (2000) and is the default method (Figure 1) in USDA-ARS BSTEM Version 5.4. This method was developed specifically for bank failure applications and is derived superficially to compute failure planes through vertically heterogeneous bank

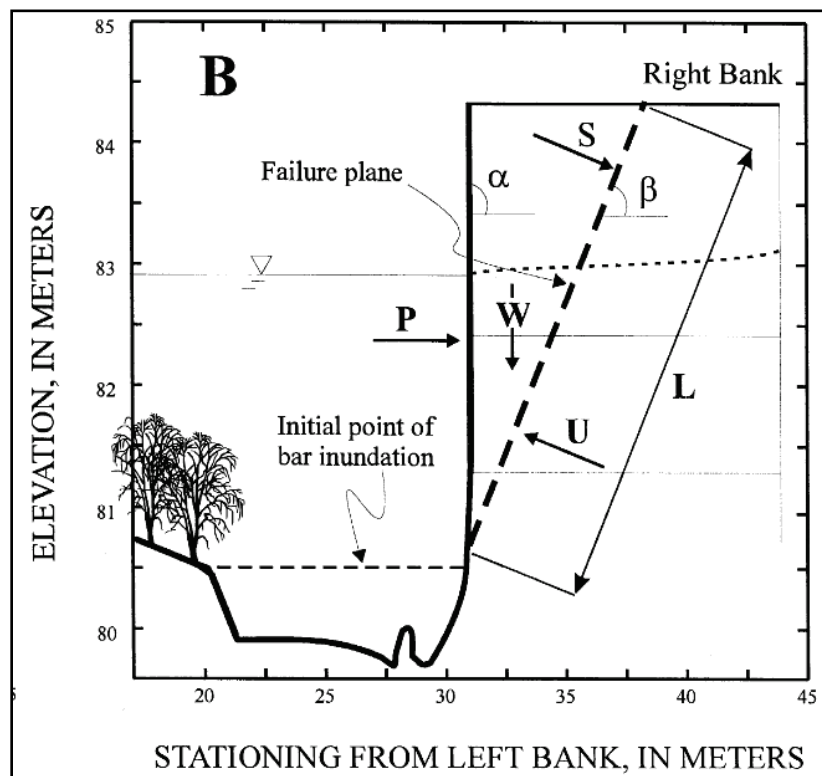


Figure 1. Force diagram for the "Layer Method" from Simon, 2000.

sediments. The layered configuration makes it easier to formulate a stability equation for bank sediments divided into discrete horizontal layers (which is the basic configuration of BSTEM stratigraphy). The Layer Method also eliminates one cycle of iteration required in the Method of Slices, which reduces runtimes in long simulations.

The Layer Method solves a non-iterative equation (Equation 1, Layer Method Force Balance) for the FS that compares driving forces to resisting forces:

$$FS = \frac{\sum_{i=1}^I (c'_i L_i + S_i \tan \phi_i^b + [W_i \cos \beta - U_i + P_i \cos(\alpha - \beta)] \tan \phi_i')}{\sum_{i=1}^I (W_i \sin \beta - P_i \sin[\alpha - \beta])} \quad (1)$$

where:

- i = layer
- L = length of the failure plane
- S = matrix suction force
- U = hydrostatic uplift
- P = hydrostatic confining force of the water in the channel
- ϕ' = friction angle
- ϕ^b = relationship between matrix suction and apparent cohesion
- c' = effective cohesion
- b = angle of the failure plane

However, Equation 1 combines the driving forces in the numerator and resisting forces in the denominator, because both the numerator and denominator have negative components. Equation 2 displays the components of the Layer Method Force Balance equation, with the driving forces indicated in red and resisting forces in green.

$$FS = \frac{\sum_{i=1}^I \left(\underbrace{c'_i L_i}_{\text{Cohesion}} + \underbrace{S_i \tan \phi_i^b}_{\text{Suction}} + \underbrace{[W_i \cos \beta - U_i + P_i \cos(\alpha - \beta)]}_{\substack{\text{Frictional Resistance} \\ \text{Weight of the soil} \quad \text{Hydrostatic uplift} \quad \text{Confining force normal to failure plane}}} \tan \phi_i' \right)}{\sum_{i=1}^I \left(\underbrace{W_i \sin \beta}_{\substack{\text{Gravitational force along the inclination of the failure plane}}} - \underbrace{P_i \sin[\alpha - \beta]}_{\substack{\text{Hydrostatic confining force acting against the weight}}} \right)} \quad (2)$$

The forces in Equation 2 can be categorized into soil forces (weight of soil block, cohesion) and hydraulic forces (hydrostatic confining forces, pore water pressure). Equation 3 distinguishes the hydraulic and soil forces of the Layer Method Force Balance equation:

$$FS = \frac{\sum_{i=1}^I \left(\overset{\text{Soil}}{c'_i L_i} + \overset{\text{Hydraulic}}{S_i \tan \phi'_i} + \left[\overset{\text{Soil}}{W_i \cos \beta} - \overset{\text{Hydraulic}}{U_i} + \overset{\text{Hydraulic}}{P_i \cos(\alpha - \beta)} \right] \tan \phi'_i \right)}{\sum_{i=1}^I \left(\overset{\text{Soil}}{W_i \sin \beta} - \overset{\text{Hydraulic}}{P_i \sin[\alpha - \beta]} \right)} \quad (3)$$

TR.1.1.1 Soil Forces

Weight of the Soil in the Failure Block

The weight of the soil in the failure block is an instrumental parameter in both the driving and resisting forces. The gravitational force on the mass of the bank "inside" of the failure plane is the primary driver of bank failure. However, the component of this weight normal to the failure plane also increases the frictional resistance to failure.

$W_i \sin \beta$ = The component of the weight down the failure plane, driving the soil into the water.

$W_i \cos \beta \tan \phi'_i$ = The frictional resistance of the soil along the failure plane, where:

$W_i \cos \beta$ = component of the weight normal to the failure plane

ϕ'_i = friction angle (which can be measured in the laboratory with triaxial testing or *in situ* with borehole shear equipment).

Cohesion

Cohesion is the inter-particle attraction in a soil matrix. For very fine soils (generally less than 0.0625 mm), particularly those composed of clay minerals, the electrochemical forces between particles can be stronger than the frictional forces. These electrochemical binding forces resist failure in cohesive soils such that:

$c'_i L_i$ = The effective cohesion per unit length (c'_i) acting along the length of the failure plane in a soil layer L_i . (Note: cohesion is actually a shear strength that acts over an area, but L_i becomes an area when it is projected along the stream wise or longitudinal direction).

TR.1.1.2 Hydraulic Forces

For hydraulic forces there are two terms that consider the weight of the water and two terms that consider the pore water pressure.

Hydrostatic Confining Forces

The terms that consider the force of the water in the channel:

$P_i \cos(\alpha - \beta) \tan \phi'_i$ = The normal component of the hydrostatic confining force of the water in the channel. This is a resisting force because it adds to the normal force acting on the failure plane and, therefore, increases the frictional strength.

$-P \sin(\alpha - \beta)$ = The component of the hydrostatic confining force acting along the failure plane against the direction of failure. The weight of the soil (the primary driving force) is reduced by this component.

α = is the angle between vertical and the vector the hydrostatic force (Figure 2) exerted by the channel water (orthogonal to the weighted average of the inundated bank slope) are both resisting forces

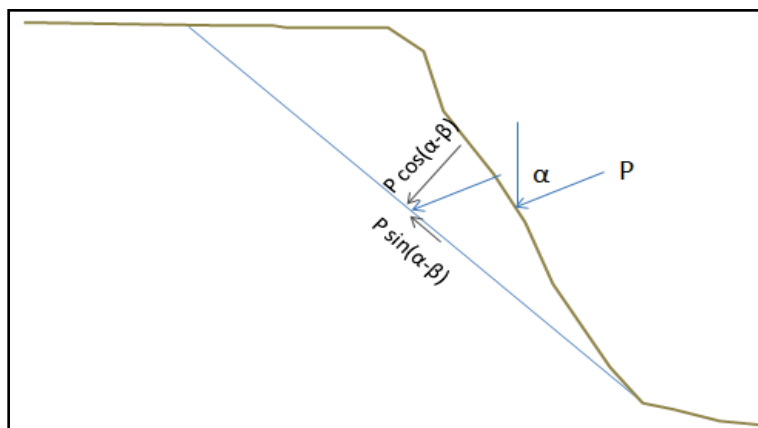


Figure 2. Components of the hydrostatic forces acting normal to and along the failure plane.

Pore Water Pressure

The pore water pressure is divided into two components in the numerator:

$-U_i \tan \phi'_i$ = Hydrostatic uplift force (buoyancy is a driving force while suction is a resisting force). Water exerts a vertical force on submerged sand grains, reducing the normal force along the failure plane and, therefore, the frictional resistance to failure. U_i is simply the hydrostatic force, which increases linearly with depth below the groundwater table (Figure 3). In the saturated zone $\phi_b = \phi'$ so the hydrostatic force is multiplied by $\tan \phi'$ and can be included in the frictional term of the numerator.

$S_i \tan \phi_i^b$ = The suction forces increase the soil strength due to the development of negative pore water pressure in the unsaturated zone of the soil which pulls the soil grains together. In the unsaturated zone, as water drains, evaporates, transpires, and is not replaced with atmospheric air, negative pressures (suction) develop.

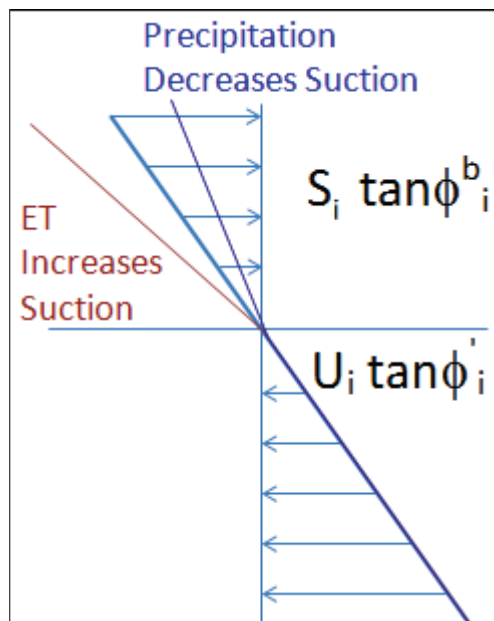


Figure 3. Idealized hydrostatic assumption of positive and negative pore water pressure with respect to the groundwater surface and potential empirical divergence from the assumption.

In general, suction S_i is estimated as a continuation of the hydrostatic force into the unsaturated zone. Suction increases with vertical distance above the water table at the same rate that the hydrostatic force increases with vertical distance below the water table. Positive and negative pore water pressures are assumed symmetrical around the water table. This is an idealized assumption, however, that only accounts for gravity draining. Precipitation and infiltration will add water to the unsaturated zone and decrease suction effects and evapotranspiration will increase negative pore water pressures. If these processes are important, unsaturated pore water pressures will have to be measured (e.g., with a tensiometer).

Translating negative pore water pressures or suction effects into a force in the free body diagram is the most empirical step of computing the factor of safety. Every other parameter can be measured directly or computed. However suction effects are accounted for with an empirical assumption analogous to the friction slope parameter. The suction is translated into "apparent cohesion", (the equivalent amount of cohesion required to produce the same resisting force as the soil suction). Apparent cohesion (Figure 4) is easily included in the force balance, but is not a physical parameter that can be measured and is very difficult to compute. The angle ϕ^b is simply the linear relationship between the matrix suction measured or computed and the corresponding equivalent cohesion force it represents. This angle can be computed but is heavily labor and data intensive to measure so it is often selected based on user judgment. For most materials ϕ^b is generally between ten to thirty degrees depending on soil type. Most applications use a base ϕ^b between ten and fifteen, but it goes to a maximum of the friction angle when the material is saturated (Fredlund, 1996). Since it is one of the least certain parameters it is often considered a calibration parameter.

If the water surface in the channel is close to the groundwater elevation the confining forces of the water in the channel offset most of the driving force of the interstitial water. However, if the

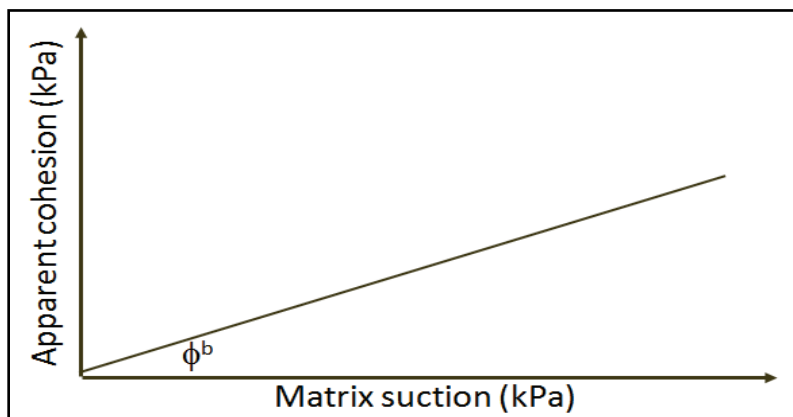


Figure 4. Relationship between measured or computed matrix suction and the empirical strength "apparent cohesion" defined by the ϕ^b parameter.

water in the channel is substantially lower than the soil water elevation (e.g., in the case of a rapid channel drawdown in poorly drained soils, leaving a perched groundwater table), the confining forces of the water will be removed while the driving forces (the weight of the water and the buoyant reduction in soil friction) remain. This is why the **critical failure condition** is often a case of substantial differential between groundwater and surface water elevations.

TR.1.2 Method of Slices

The Method of Slices algorithm included in HEC-RAS follows the more classical geotechnical approach to planar failure. The formulation of the method of slices for bank failure analysis comes from Langendoen (2008). Before the analysis the algorithm divides each user specified material layer into vertical slices of equivalent width (Figure 5). This ensures that the force and momentum balance computed for each segment of the failure plan will not include more than one material type.

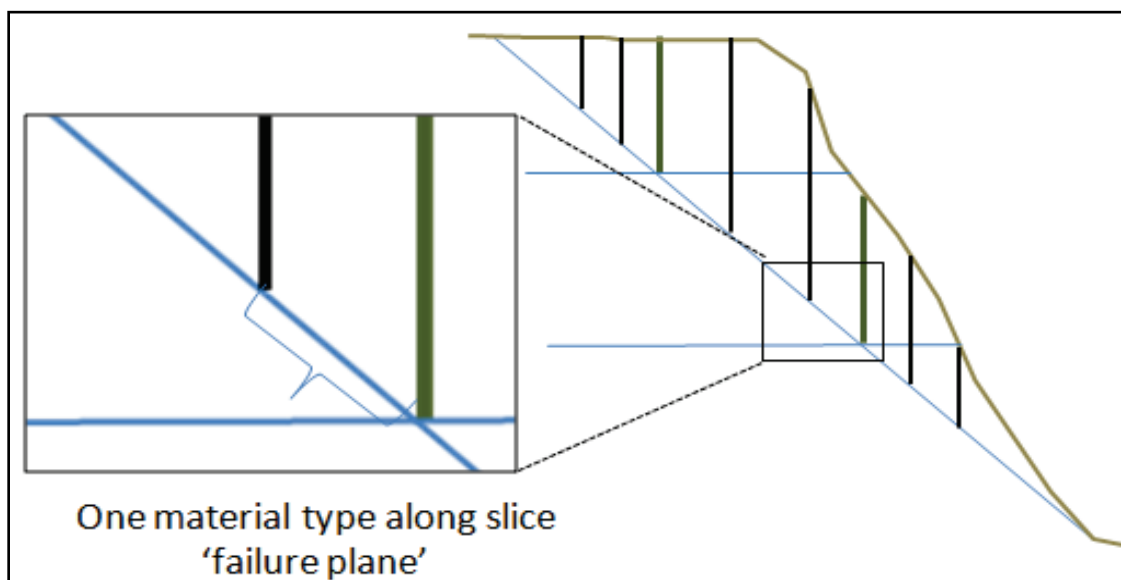


Figure 5. Subdivision of layers into slices. The failure block through each layer is divided into three slices of equivalent width.

The initial formulation of the method of slices (Bishop, 1955) considered forces acting at the base of each slice (along the failure plane) and included force (Figure 6) and momentum balances that were both vertical and normal to the slip surface. Morgenstern and Price (1965) added inter-slice forces in their analysis of earthen dams. The algorithms in USDA-ARS BSTEM for HEC-RAS include both inter-slice forces. The forces that act on each slice include: the weight of the slice W_j , the normal force acting on the base of the slice N_j , the shear force induced at the base of the slice S_j , inter-slice normal forces E_j , and the vertical shear forces between slices X_j .

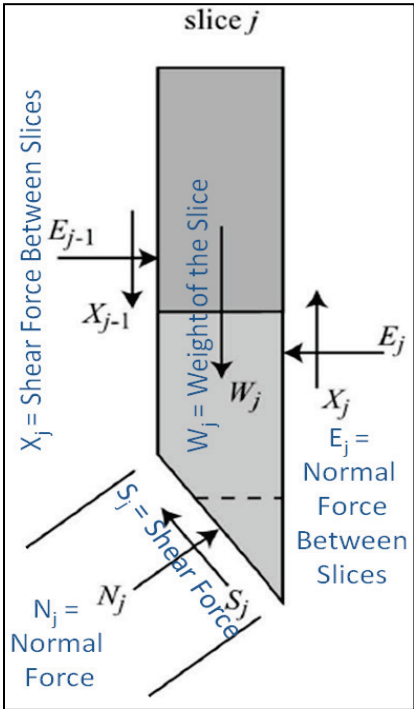


Figure 6. Forces acting on a slice.

E_j and X_j = The inter-slice normal (E_j) and shear (X_j) forces are unique to the method of slices and deserve attention before the algorithm is described. Calculating inter-slice normal forces (E_j) from a horizontal force balance on the slice is relatively straight forward (Equation 4, Inter-slice Shear Forces). However, there is not an elegant theoretical approach to computing inter-slice shear forces. Stress-strain soil data demonstrate that there is a reasonably reliable empirical relationship of the ratio of inter-slice normal (E_j) and shear (X_j) such that:

$$X_j = \lambda E_j f(x) = 0.4 E_j \sin(\pi x / L_x) \tag{4}$$

where:

- λ = the maximum ratio (forty percent),
- $f(x)$ = a non-linear function between zero (0) and one (1) that apportions the ratio spatially,
- x = the lateral distance into the bank
- L = lateral width of the failure plane

In other words, at its maximum (in the center of the failure block) the shear force is forty percent of the normal force (Figure 7), and the shear-to-normal ratio decreases for slices farther from the center and closer to the margins.

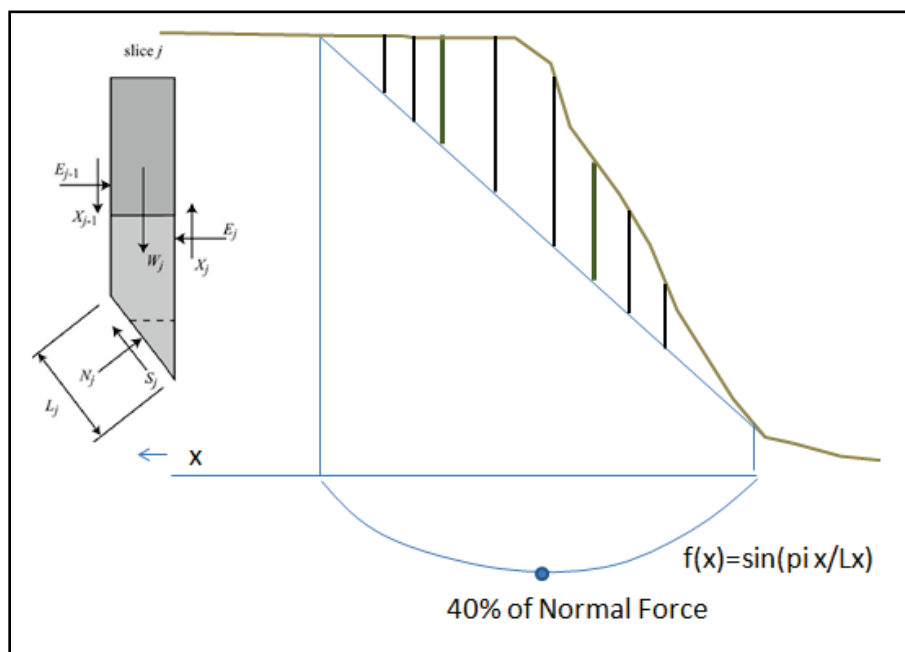


Figure 7. Schematic of how the ratio of inter-slice shear stress to inter-slice normal stress ($\lambda=0.4$) is reduced by $f(x)$ depending on the proximity of the slice to the center of the failure block.

FS can be computed by summing (for all slices, j) the forces acting along the failure plane. The equation for computing FS along the failure slope is a familiar mix (from the Layer Method) of driving (red labels) and resisting (green labels), soil (brown circles) and hydraulic (blue circles) forces in Equation 5 (Force Balance).

$$\text{FS} = \frac{\text{Cohesion} \quad \text{Frictional resistance} \quad \text{Hydrostatic uplift}}{\sec \beta \sum_{j=1}^J \left(L_j c'_j + N_j \tan \phi'_j + U_j \tan \phi_j^b \right)} \tag{5}$$

$$\frac{\tan \beta \sum_{j=1}^J \left(W_j - F_w \right)}{\text{Weight of soil} \quad \text{Hydrostatic confining force}}$$

where:

- FS = factor of safety
- U = hydrostatic uplift
- P = hydrostatic confining force of the water in the channel
- ϕ' = friction angle
- ϕ^b = relationship between matrix suction and apparent cohesion
- c' = effective cohesion
- W = weight of the soil
- F_w = hydrostatic confining force

This is the Bishop (1955) approach that accounts only for the forces native to the individual slice. However, the normal force at the base of the slice is not a function of the forces intrinsic to the slice itself. The normal force is modified by the inter-slice normal forces on either side (E_j and E_{j-1}) or the inter-slice shear (X_j and X_{j-1}) on either side of the slice. An iterative solution including two additional equations is required to compute these effects.

The inter-slice forces are calculated from the horizontal force balance (Equation 6, Horizontal Force Balance) for the slice:

$$E_j - E_{j-1} = [W_j - (X_j - X_{j-1})] \tan \beta - (c'_j L_j + N_j \tan \phi'_j - U_j \tan \phi_j^b) \frac{\sec \beta}{FS} \tag{6}$$

Equation 6 has FS imbedded and uses the FS computed in Equation 5. With FS being computed in Equation 5, and the shear forces between neighboring slices (X_j and X_{j-1}) coming from Equation 6, a Normal force at the base of the slice that is modified for inter-slice effects, can be computed from the vertical force balance (Equation 7) of the slice:

$$N_j = \frac{W_j + X_{j-1} - X_j - (L_j c'_j - U_j \tan \phi_j^b) \frac{\sin \beta}{FS}}{\cos \beta + \frac{\tan \phi'_j \sin \beta}{FS}} \tag{7}$$

The new normal force at the base of the slice is then substituted back into Equation 5 to compute a new FS, which is used to update the inter-slice forces in Equation 6 and to update the Normal force in Equation 7. The Method of Slices iterates on these three equations (Figure 8) until the change in FS between iterations drops below 0.5 percent.

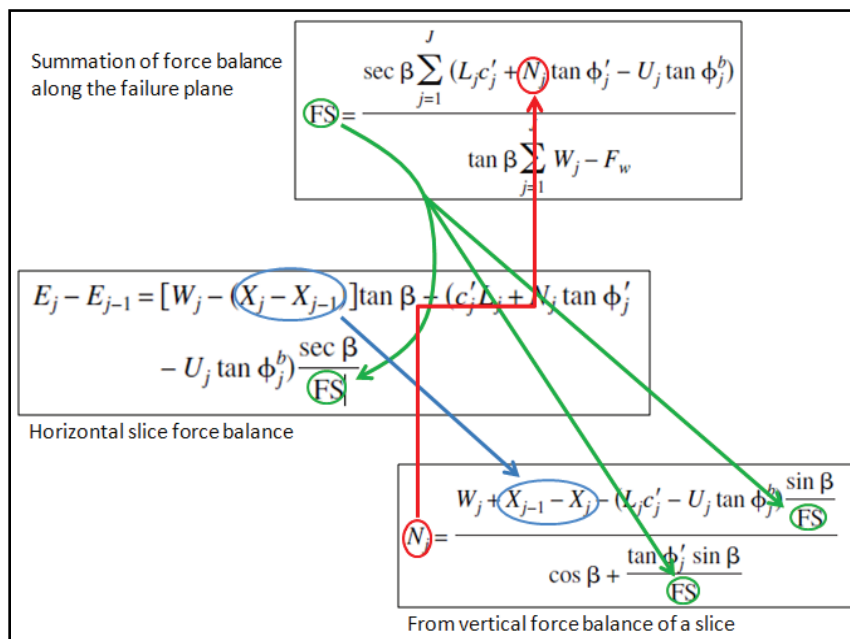


Figure 8. Iterative scheme to compute FS for the method of slices including the dependency of the normal force at the base of the slice on the inter-slice forces.

There are some considerations in the code to decrease the computational expense of iteration. The code checks the denominators of the equations for FS and N_j to determine if iteration is necessary.

TR.1.2.1 Tension Cracks

Tension cracks are a special case of the Method of Slices computation. Because of the vertical nature of tension cracks, tension cracks can only be computed by the Method of Slices. The USDA-ARS standalone version of BSTEM uses the Layer Method by default but switches to the Method of Slices if the tension crack parameter is defined and a tension crack is identified.

If the inter-slice normal forces are negative "E less than zero" the slice is in "tension". Soil generally performs very poorly under tension. Tension slices tend to be on the "upslope" portion of the failure block because there is more material "sliding away" pulling on the slice. Therefore, the code starts at the (channel side) and works inland, checking each slice interface for "E less than zero".

When a slice in tension is found, the software compares the height of the slice interface to the user specified (or internally calculated) "maximum tension crack depth". If the slice interface is greater than maximum tension crack, then no tension crack is computed at that location and the next inland interface is analyzed. Therefore the tension crack happens at the slice interface closest to the channel that fulfills the two following criteria:

- 1) E less than zero (i.e., the slice interface is "in tension")
- 2) The height of the interface between the slices is less than the maximum tension crack (Figure 9)

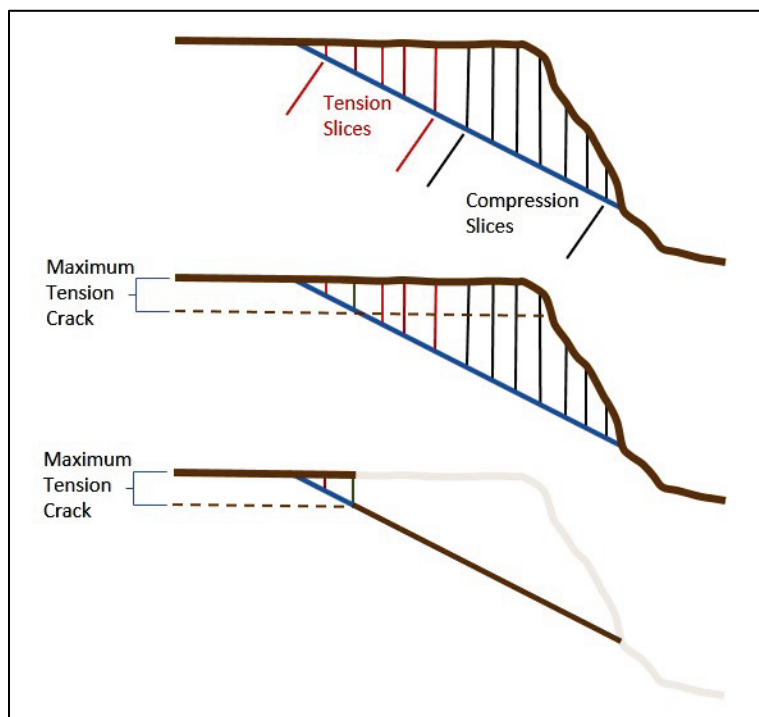


Figure 9. Tension crack computation criteria.

The vertical thickness of tension cracks is soil specific and can be determined by visual field inspection of the vertical cut at the upper portion of existing bank failures. Tension cracks vertical thickness can also be computed with Equation 8 for the depth at which active pressure goes to zero (Lambe, 1969):

$$z_c = \frac{2c'}{\gamma} \tan(45^\circ + \phi' / 2) \quad (8)$$

HEC-RAS currently uses Equation 8 by default for the method of slices. The standalone version of BSTEM can override this value with a user specified maximum tension crack, but this is not available in HEC-RAS at this time.

If a tension crack is identified, the slices inland from the tension crack are excluded from the stability analysis. Because the failure plane along these inland slices is higher, the inland slices will tend to have higher suction forces and lower buoyant forces. Therefore, a tension crack that excludes these inland slices will reduce the FS and make the bank more likely to fail.

If FS is less than zero and a tension crack is computed, the failure block on the river side of the tension crack is removed from the bank and added as sediment load to the sediment model, while the inland slices remain fixed to the bank, resulting in a vertical wall.

TR.1.2.2 Cantilever Failures

Cantilever failures, mass wasting of overhanging soil blocks, are also a special case of the Method of Slices. Thorne and Tovey (1981) established three types of cantilever failures (Figure 10) that include three distinct processes:

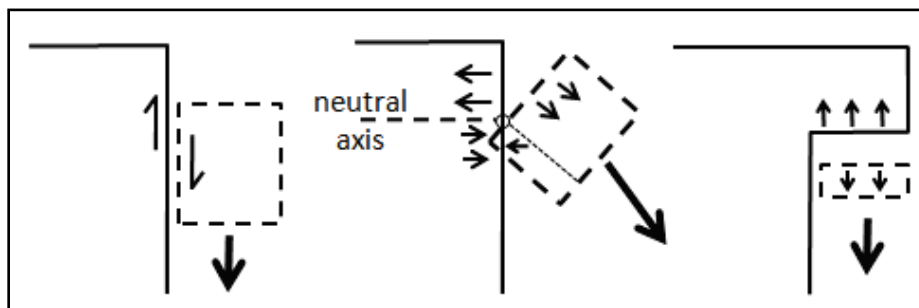


Figure 10. A taxonomy of cantilever failure mechanisms (after Thorne and Tovey, 1981).

1. The soil block shears off along the vertical or obtuse failure plane.
2. The soil block rotates off the bank due to the tension (e.g., inter-slice normal forces go to zero and cohesion is not sufficient to keep the overhanging block in place).
3. The lower layer of the block falls off.

There is no special cantilever case algorithm in HEC-RAS. The methods available in HEC-RAS can only apply the Method of Slices to overhanging bank configurations, and therefore can only simulate the first (sliding) mechanism of cantilever failure. Ninety degrees is the maximum failure angle that HEC-RAS will consider.

To identify cantilever failure, HEC-RAS checks to see if the maximum β (the maximum failure plane angle that is entirely included in the bank soil) at any evaluation point is greater than or equal to ninety degrees (Figure 11). This indicates an overhanging bank and that Method of Slices was used for the evaluation at that point even if the Layer Method is selected.

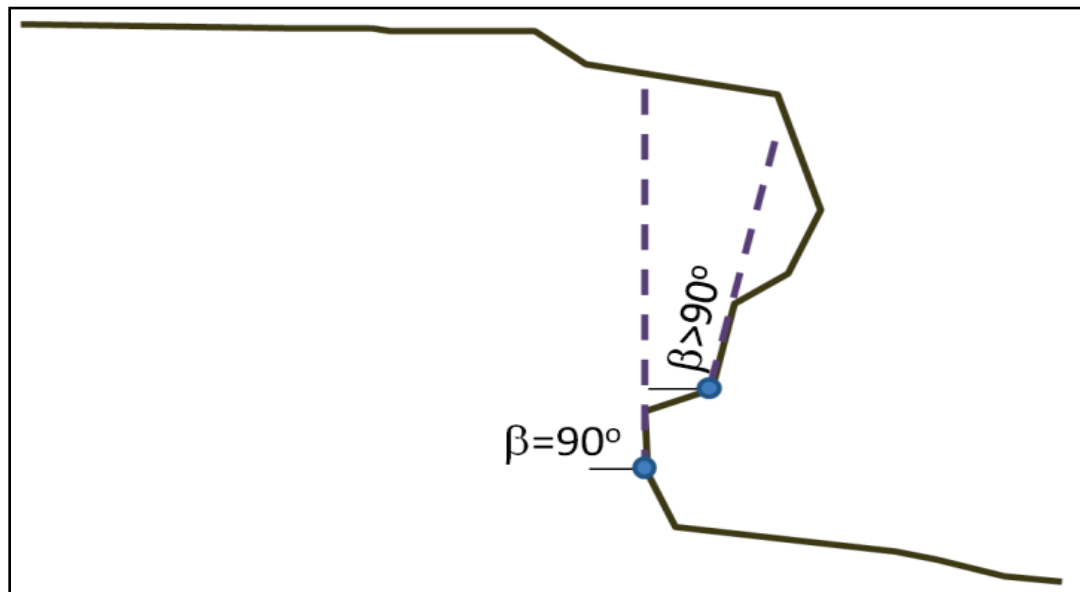


Figure 11. Example of maximum failure plane angles for overhanging bank situations where β_{\max} is greater than or equal to ninety degrees. These classify as cantilever failures and the software will force a Method of Slices analysis.

TR.1.3 Selecting a Method

The Layer Method and the Method of Slices generally produce very similar results. Differences between the two methods are summarized in Table 1. The standalone version of the USDA-ARS BSTEM model uses the Layer Method unless it has to compute tension cracks or cantilever failure, which cause it to switch to the Method of Slices. The choice mainly involves a trade-off between a theoretical consideration (the normal force distribution) and a practical consideration (run time).

Table 1. Method selection criteria

Layer Method	Method of Slices
Customized for bank failure applications.	Closer to the comparable geotechnical analyses.
Higher normal stresses along the failure plane generally computed for the higher layers.	Higher normal stresses along the failure plane generally computed for the deeper layers.
Non-Iterative. More computationally efficient.	Apportions normal stresses according to more physically based assumptions.
Switches to method of slices if tension cracks or overhanging banks form.	Computes tension crack and cantilever failures.

Method of Slices computes a somewhat more realistic distribution of normal stresses along the failure plane (Figure 12). The Layer Method computes larger normal stress for larger layers, which tend to be along the top of the failure plane while the Method of Slices computes larger normal stresses for larger slices which tend to exert their forces at the base of the failure plane

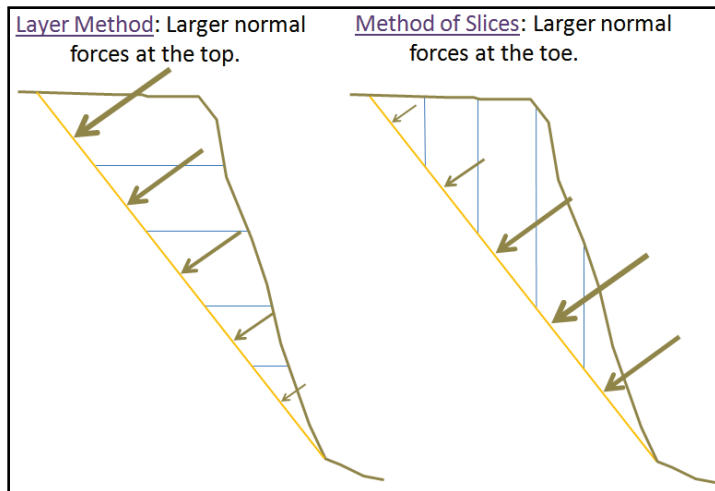


Figure 12. Theoretical difference in normal stress computed by Layer Method and Method of Slices.

(which is a more realistic assumption). Therefore, without tension cracks, the Method of Slices will generally compute a slightly higher FS for the same dataset. However, because the Method of Slices allows tension cracks, which tend to remove more resisting forces than driving forces, the Method of Slices often returns a lower FS, and more failures.

However, because the Method of Slices is iterative and the Layer Method is not, the Layer Method is more computationally efficient and can decrease run times. Since there are already two iterative computations in BSTEM outside of the FS computation (e.g., analysis for several nodes up the bank face and the selection of the critical failure plane for each node) bank failure analysis can be computationally expensive for big projects or long runs. The Layer Method may reduce those run times.

TR.1.4 Steps in a Bank Failure Analysis

The physics described in the sections above, computes FS for a single failure plane. However to determine if the bank will fail and where it will fail several failure planes 1) with different starting elevations on the face of the bank, and 2) with different angles have to be evaluated (Figure 13).

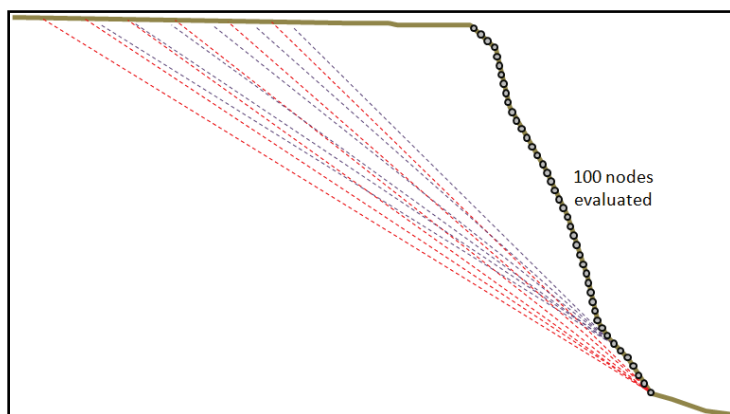


Figure 13. Multiple failure planes have to be evaluated at multiple nodes.

Therefore, regardless of what method was used to compute the physical FS, the following is a six step iterative evaluation for each bank and time step analyzed:

1. Evaluate nodes at several vertical locations up the bank. Then for each node follows Step 2 through 6.
2. Select the bounding failure planes (minimum and maximum angles) and an initial guess for the critical factor of safety - FS_{cr}
3. Compute the factor of safety for the current proposed failure plane - FS_i
4. Use that information to select a more likely critical failure plane (using the "bracket and Brent" optimization algorithm) ($FS_{i+1} \rightarrow FS_{cr}$)
5. Decide when FS is close enough to FS_{cr} to stop, otherwise repeat Step 3
6. Select the FS_{cr} for all nodes and if FS_{cr} is less than one, fail the bank, update the cross section, and send the bank sediments to the routing model

The following describes the above steps in more detail.

1. Evaluate nodes at several vertical locations up the bank

The software will find a critical failure plane that starts at several vertical locations along the face of the bank. HEC-RAS evaluates 100 points which are evenly spaced vertically between the user specified toe and top of bank (one percent evaluation intervals) by default. Fewer evaluation points can be specified under BSTEM to improve run time. However, bank points that are evenly spaced will not be evenly spaced along an irregular bank.

For each elevation, the bank failure algorithms will find a critical FS failure plane. Instead of running many angles for each node at very small increments, a minimization algorithm with quadratic convergence "bracket and Brent" (Teukolsky, 2007; page 388) is used to find the failure plane with the minimum FS at each node with as few failure planes as possible. This process includes the next Steps 2 through 6.

2. Select the bounding failure planes (minimum and maximum angles) and compute a FS for each

The first step of finding the critical FS of a given bank node is to bound the possible angles (the "bracket" in "bracket and Brent"). The minimum angle is set to half of the friction angle, which is a reasonable angle below which most bank configurations would be expected to remain stable. The maximum angle is the largest angle that is entirely in the soil matrix (Figure 14).

Then the bank failure method makes an initial guess for the critical failure plane to start the parabolic search, which is 45 degrees plus half the friction angle.

However, sometimes it is not as simple as the classical configuration in Figure 14. A number of unique configurations posed by natural channel banks can cause the default maximum angle to be less than half the friction angle or can generate an initial guess ($45^\circ + \phi/2$) to fall outside of the bracket among other complications. Therefore, there are special cases to deal with unique configurations.

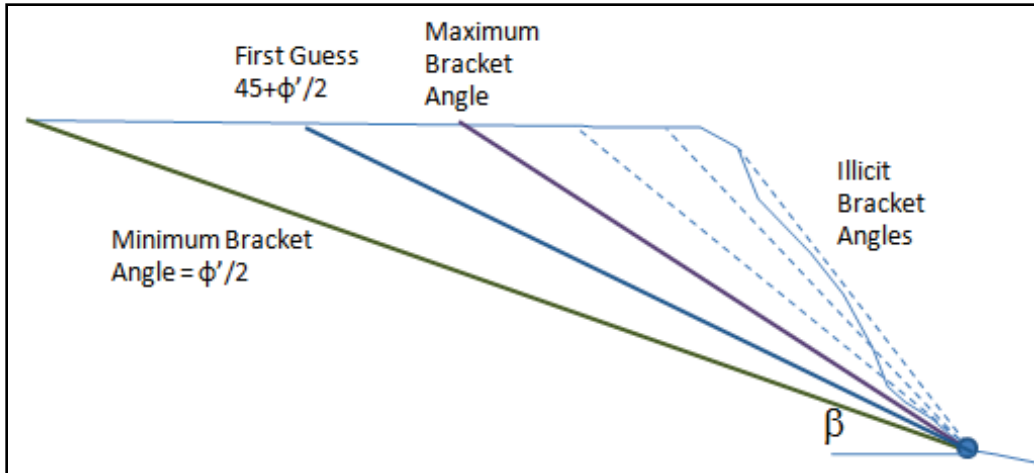


Figure 14. Computing the maximum and minimum failure angles and the first guess.

With the maximum and minimum angles set and a first estimate established, the bank failure algorithm is prepared to start the iterative search to determine a critical failure plane angle.

In the initial iteration, an FS is computed for the maximum, minimum, and initial estimate failure plane angles by the methods described above (Figure 15). In each successive iteration, an FS is computed for the new failure plane angle selected by the parabolic search.

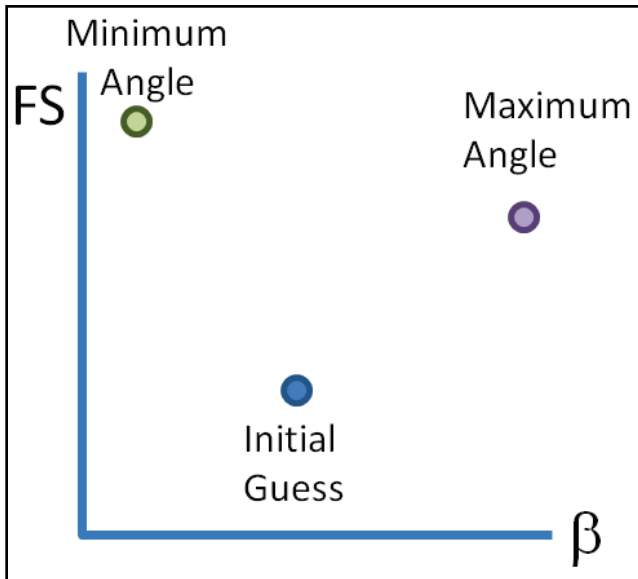


Figure 15. FS computed for the maximum and minimum angles and the initial estimate

FS is computed for the maximum, minimum and best guess angles with the physics described above, and then the three angle-FS pairs are passed to the "bracket and Brent" routine, which fits a parabola to the FSs associated with the three angles and then iterates to find the minimum. With each iteration, the bracket shrinks (the maximum and minimum possible angles converge) and the algorithm completes when the bracket drops below 0.5 degrees.

3. Compute FS_i

The algorithm computes an FS for the β_i selected by the methods described in Step 2.

4. Use that information to select a more likely critical failure plane

Next HEC-RAS uses a parabolic optimization algorithm ("bracket and Brent") to find an angle (β) that is likely to have a lower FS. The software fits a second order quadratic equation through the three factors of β - FS points and identifies the angle (β_i , Figure 16a) associated with the parabolic minimum.

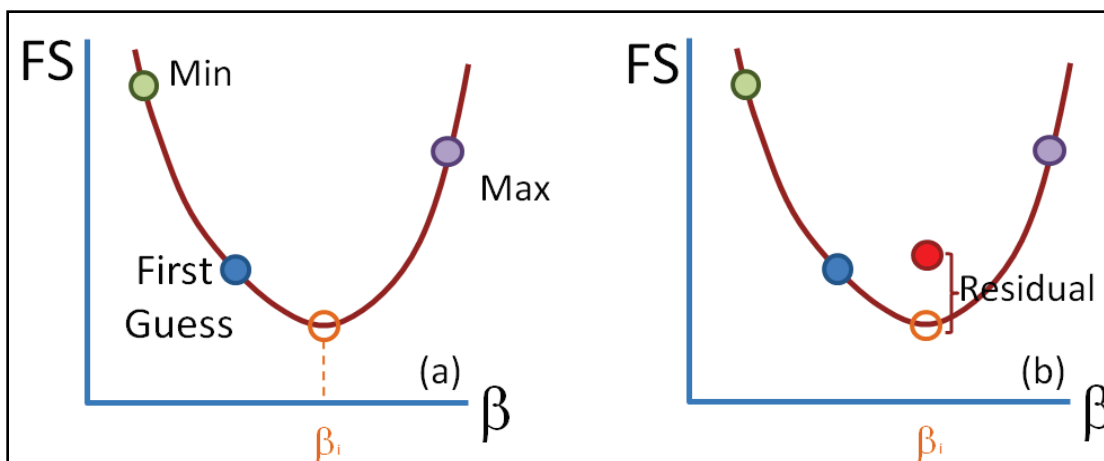


Figure 16. A parabolic function is fit to the three points and a) the function minimum is selected as the next failure plane, and b) compute a FS associated with that failure plane and the residual between the FSs predicted by the method.

5. Decide when the FS is close enough to FS_{cr} to stop, otherwise Iterate

The actual relationship between β_i and FS does not necessarily fit a second order quadratic equation. Therefore, the FS computed for the angle selected (β_i) will not precisely match that predicted by the function. The bank failure algorithm evaluates the difference between the computed FS and the predicted FS ("Residual", Figure 16b). If the difference is less than half a percent (i.e., residual less than 0.5 percent) then the algorithm considers the parabolic function a good approximation of the relationship between FS and β and the β_i is adopted as the critical failure plane for this bank node.

However, if the residual is greater than 0.5 percent, the algorithm will iterate and return to Step 3, by trying to identify the most likely critical failure plane angle given the new information. The new FS_i for the new β_i becomes the new maximum or minimum (depending on which side the last β_i is on) and a new, narrower, second order quadratic is fit to the new three points (Figure 17). A new β_{i+1} is selected at the minimum of the function. The FS is calculated (Step 4) and the residual evaluated (Step 5). As this algorithm iterates the range between the maximum and the minimum shrinks as the function converges (usually within a few iterations) to a solution.

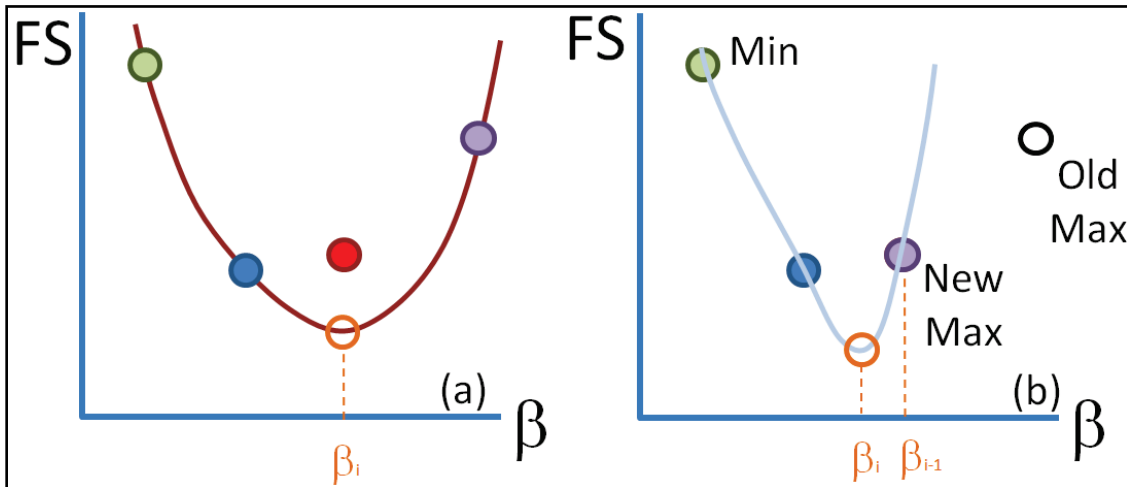


Figure 17. The new FS computed for β_i becomes the new maximum or minimum and a tighter polynomial is fit to the new three points to identify a new function minimum.

However, sometimes the relationship between β and FS depart substantially from the parabolic model, which can return false, local minimums. For example, the theoretical function in Figure 18a passes through the same points as Figure 17b but would not be predicted by the "narrowing parabolic" method. Therefore, the iteration optimization includes occasional searches to find other β regions with low FSs.

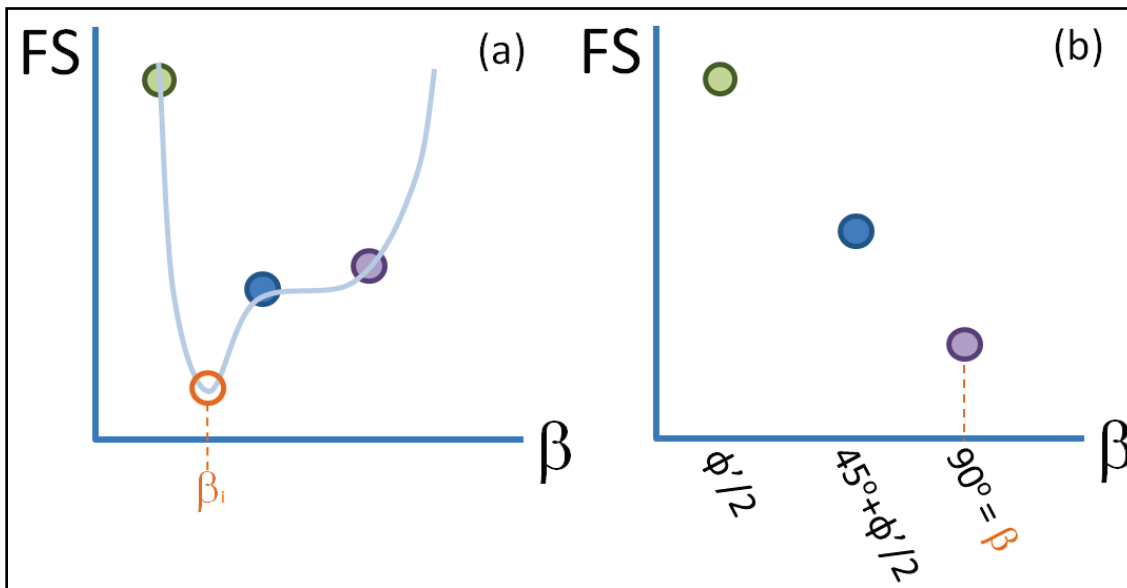


Figure 18. Monotonic β - FS function associated with a cantilever failure.

Additionally, sometimes the relationship between β and FS is monotonic (Figure 18b). This occurs in the case of cantilever failures where the highest factor of safety is often associated with the maximum angle. If the maximum angle has the lowest factor of safety in Step 2, this is automatically accepted as the critical failure plane and the model does not iterate.

6. Select the FS_{cr} for all nodes and if FS_{cr} is less than one, fail the bank, update the cross section, and send the bank sediments to the routing model

Finally, after the critical failure plane is iteratively computed for each of the vertical evaluation points on the bank, the failure plane with the lowest overall failure plane is selected. If the FS is greater than one, the bank is stable. However, if the FS is less than one, then the bank fails and the bank material inside of the failure plane is removed from the bank and added to the control volume of the sediment routing model associated with the cross section. The material inside of the failure plane is removed, the cross section is updated, and the material is introduced into the sediment routing model as a lateral load.

TR.2 Toe Erosion (Fluvial or Hydraulic Erosion) – Flow Driven

The combination of vertical bed change algorithms in the classical HEC-RAS mobile bed computations and the bank failure algorithms can model interaction between channel incision and bank failure. As a channel incises (the potential failure plane through the new exposed toe), the bank steepens, and the FS drops. Therefore incision can induce bank failure (or conversely deposition can stabilize banks). However, a third important bank evolution process is not captured by this interaction: toe scour.

Toe scour is a fluvial, hydraulic process driven by the flow (versus bank failure which is primarily a gravity driven geotechnical process). The classical mobile bed algorithms in HEC-RAS only compute vertical movement of the bed, but hydraulic forces can undermine the toe of a bank, which can reduce the length of the failure plane (and the frictional resistance) and decrease the factor of safety of the critical failure plane faster than incision.

TR.2.1 Determining the Zone of Scour

The movable bed limits in the HEC-RAS sediment transport module define the transition between incision and scour. Inside of the movable bed limits, the channel is modified by the movable bed model (incision and deposition translated into vertical node movement). Outside of the movable bed limits, scour equations are used. Separate scour limits are not provided as a user input option because nodes should either incise or scour to avoid double counting. The model is very sensitive to the selection of these limits.

The scour equations in the USDA-ARS BSTEM that are implemented in HEC-RAS compute lateral bed change of the wetted nodes outside the movable bed limits for cohesive or cohesionless soils based on a radial shear distribution.

TR.2.2 Determining τ_{node}

Unlike channel deposition or erosion, toe scour does not affect all nodes equally. This is important for its interaction with the bank failure model because the failure plane will likely pass through the vertical location of maximum scour. However, to compute differential lateral scour, the software must compute a local shear stress for each node.

There are several ways to post process one-dimensional hydraulics to compute local shear stress. The most common is to subdivide the cross section into vertical "prisms" (blue lines, Figure 19) and compute a local shear stress based on the hydraulic radius of each one. However, the assumption of zero inter-prism friction only holds along the planes normal to the isovels (contours of constant velocity). Vertical divisions violate this assumption because they are not perpendicular to the isovels.

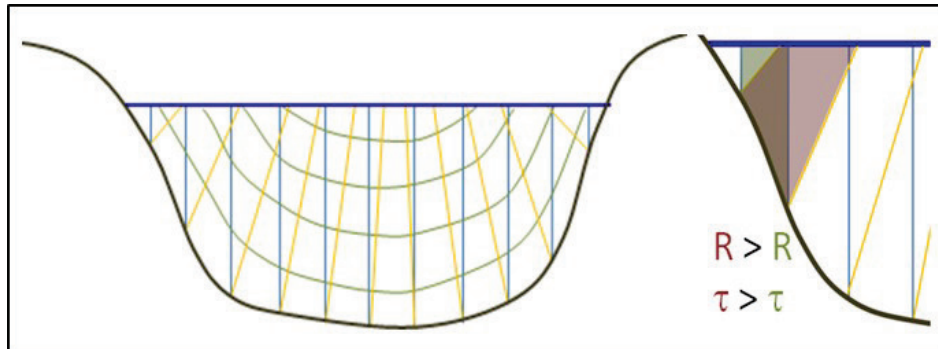


Figure 19. Subdividing the cross section into vertical conveyance prisms (blue) versus zones (yellow) perpendicular to the isovels (green).

Alternately, the one-dimensional cross section can be divided into "radial prisms", non-vertical zones by partitions perpendicular to the isovels (yellow lines, Figure 19). These approaches will compute different hydraulic radii (a sensitive variable for computing the shear stress) especially in the zone closest to the bank where the toe scour computations are applied. The radial prisms tend to have higher hydraulic radii, and therefore, higher shear stress than the vertical prism associated with the same bank segment and represent a more realistic shear stress distribution (Figure 19). Therefore, the bank erosion algorithms use a radial distribution, dividing the flow field, hydraulic radius, and shear stress with radial prisms.

If bed and bank roughness are approximately the same, then we can assume that the line that bisects the toe is normal to the isovels (Kean, 2001). Therefore, the first step in developing the radial shear distribution is finding the angle bisecting the toe (Figure 20a). Bank and channel segments are computed by connecting the scour toe (the movable bed limit) to the edge of bank and the next interior channel point respectively (Figure 20a). This segment determines the zone of the one-dimensional cross section dedicated to toe scour.

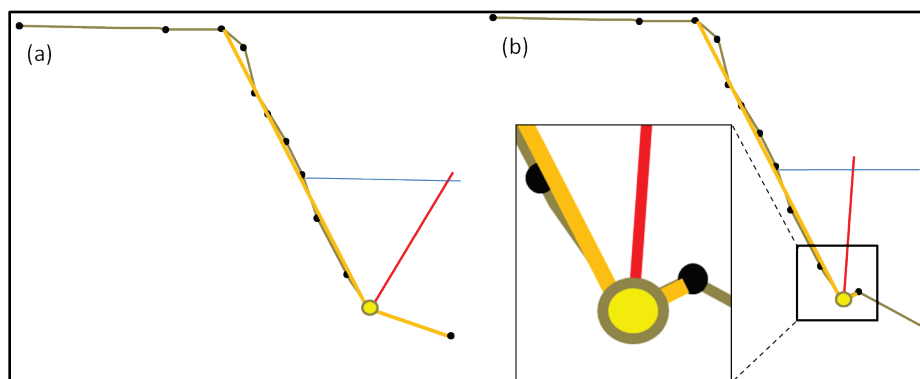


Figure 20. Finding the bisecting angle at the toe which will determine the portion of the water column that is contributing to toe scour.

Note: This computation makes the scour computations sensitive not only to the selection of the mobile bed limits but also to the elevation of the interior node. Random bed fluctuations can cause this node to diverge from the basic lateral channel slope (Figure 20b) which could artificially affect scour.

Next a "radial prism" is associated with each node (cross section station-elevation points in the toe scour zone). The water surface intersection point connects the midpoint between wetted bank nodes. The water surface intersection point is a relative proportion of the water depth of the midpoint between nodes and the total depth to the midpoint of the movable bed limit and the next interior node (Figure 21).

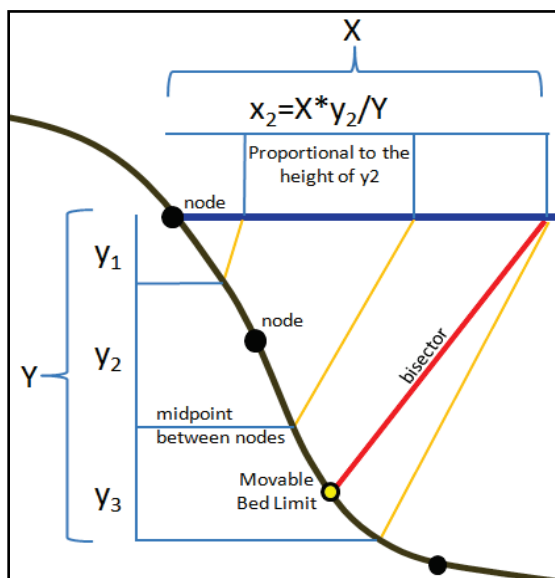


Figure 21. The orientation of the radial prisms used to compute a shear at each node is computed by proportioning the intersection of the water surface with the depth within the scour zone.

Once the radial flow prism is computed for each wetted bank node (Figure 22), the hydraulic radius of the prism is computed from the area and wetted perimeter (water-water boundaries are ignored). Then the shear stress for each radial prism is computed from the average one-dimensional shear stress as a ratio of:

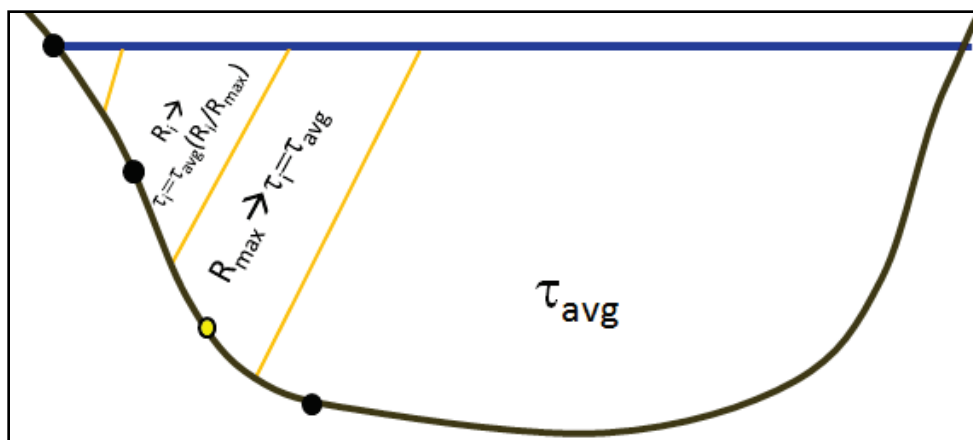


Figure 22. Apportioning the local shear by a ratio of the hydraulic radius of the radial prisms.

$$\tau_i = \tau_{avg} (R_i / R_{max})$$

where R_{max} which is typically R_{toe} is the largest hydraulic radius among the radial flow prism.

TR.2.3 Scour

If the clay content of the layer is greater than twenty percent, the software uses an excess shear cohesive equation, scoring material based on the erodibility and shear. For clay content less than twenty percent, scour is computed using a transport function. Different nodes (Figure 23) can invoke different transport equations depending on the associated layer material. Then the nodes in the toe scour region of the model are adjusted laterally.

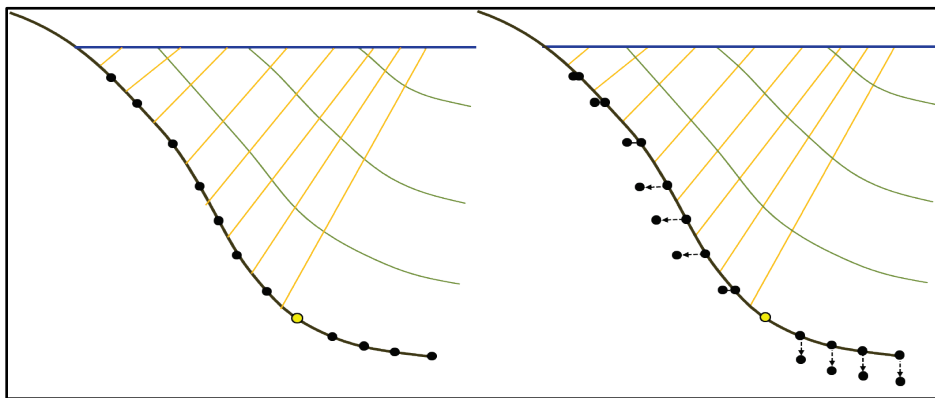


Figure 23. Nodes between the movable bed limits are adjusted vertically (and uniformly) and the wetted nodes outside the movable bed limits are adjusted laterally (and independently).

This radial shear distribution commonly computes maximum shear stress at the toe. Therefore, the toe will often scour more than the other nodes, yielding an overhanging bank like the one in Figure 24a. HEC-RAS requires increasing station values, so it cannot retain or represent overhanging banks in Version 5.0. Therefore, HEC-RAS assumes that overhanging banks fail vertically, as depicted in Figure 24b. Because overhanging banks eventually fail, this should not introduce substantial error in long term models.

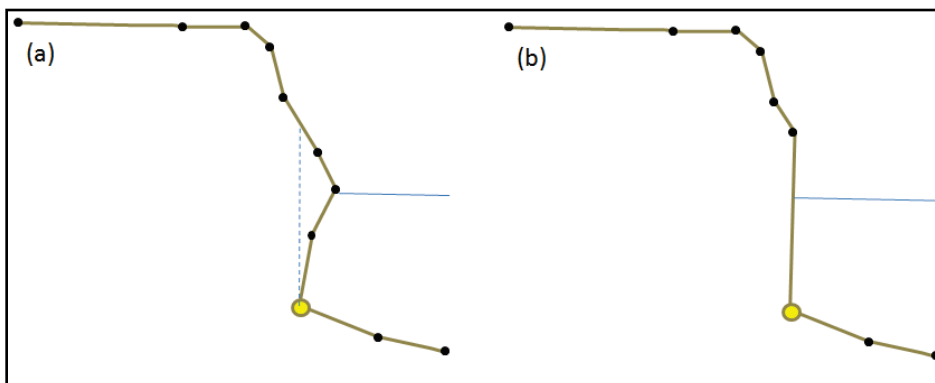


Figure 24. Overhanging bank simplification method.

USDA-ARS Bank Stability and Toe Erosion Model (BSTEM) in HEC-RAS

User's Manual

UM.1 Getting Started

BSTEM toe erosion and bank failure analysis will be performed as part of a sediment transport analysis on any cross section bank that has all the necessary parameters. Computing bank failure at every bank will increase run times. Therefore, it may be advantageous to only specify BSTEM parameters for banks that have a probability of failure. The BSTEM algorithms run before the vertical bed change algorithms each time step (i.e., HEC-RAS BSTEM cross-sections will first widen, then incise or fill).

To enter BSTEM data in HEC-RAS, from the HEC-RAS main window, from the **Toolbar**, click **Sediment Boundary Conditions** (Figure 25). Bank failure analysis is currently only computed as part of a sediment transport analysis. The **Sediment Data Editor** will open (Figure 26). From the **Sediment Data Editor** the user will enter standard sediment transport data on the first two tabs (Figure 26). To enter BSTEM information, click the **USDA-ARS Bank Stability & Toe Erosions MODEL (BSTEM)** tab (Figure 26).

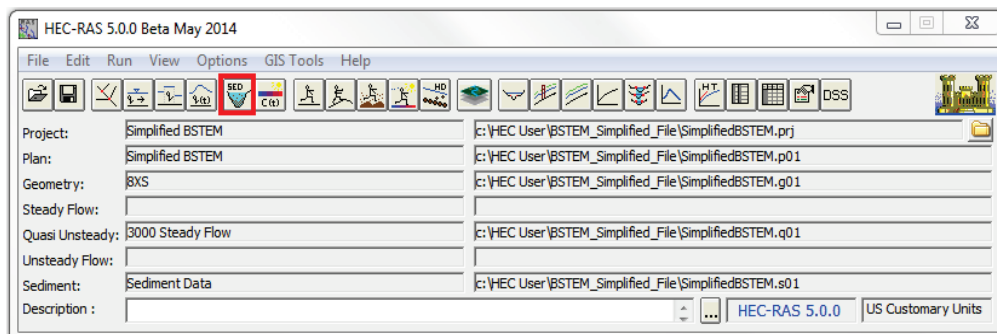


Figure 25. HEC-RAS Window.

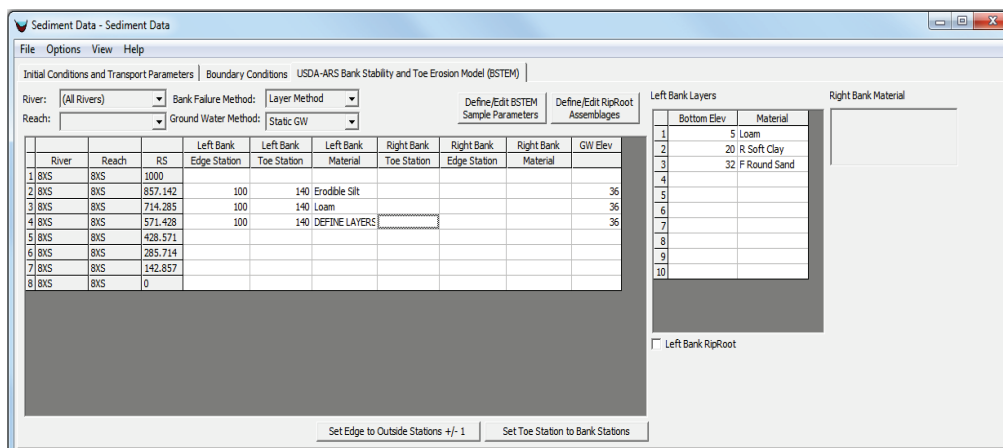


Figure 26. HEC-RAS Sediment Data Editor - USDA-ARS BSTEM Tab.

UM.2 Defining Cross Section Configuration

BSTEM can be applied to the left, right or both banks of an HEC-RAS cross section. Setting up a half-cross section (for the left or right bank) in such a way that it is also compatible with BSTEM is an extremely important step in getting physically appropriate failures from the BSTEM computations. The conceptual BSTEM half cross section (Figure 27) is composed of four segments (green labels, Figure 27) with unique slopes:

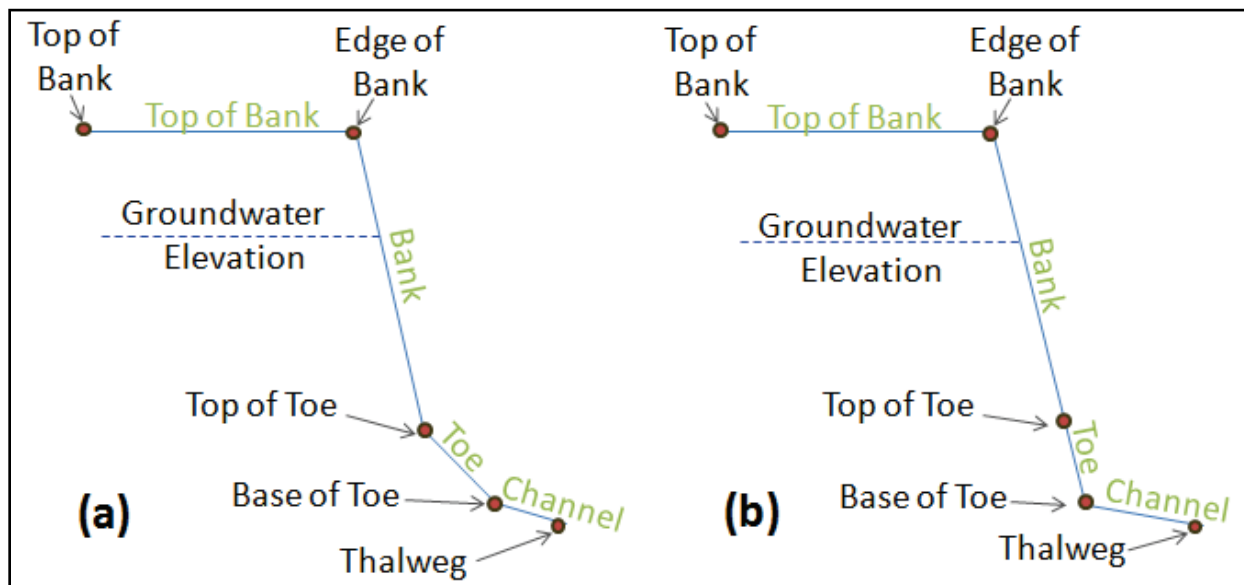


Figure 27. Definition of station points for BSTEM half cross sections

1. The **Top of Bank** which is the relatively flat portion of the cross section above the bank.
2. The **Bank** which is the steepest part of the cross section.
3. The **Toe** which is a mild slope between the bank and the channel, presumably composed of blocks of material that have fallen and accumulated at the base of the bank and are protecting the toe or some sort of rip rap or toe protection.
4. The **Channel** which is the region between the toe and the thalweg.

Each bank of each cross section BSTEM analyzes requires two user defined points, an **Edge of Bank** station and a **Top of Toe** station. These points are defined by their station across the cross section, not their elevation. These points are depicted in Figure 28 and are entered on the HEC-RAS **Sediment Data Editor** (Figure 26) and are defined below. HEC-RAS will automatically select the lowest station-elevation point in the cross section to be the **Thalweg**. HEC-RAS divides a cross section at the thalweg and uses the station-elevation points to the left of the thalweg for the left BSTEM half-cross section and those to the right of the thalweg for the right BSTEM geometry.

Left Bank Edge Station: This should be the inflection point between the bank and the top of the bank. All failure planes considered will intersect the top of bank between the edge of bank and the first cross section station-elevation point.

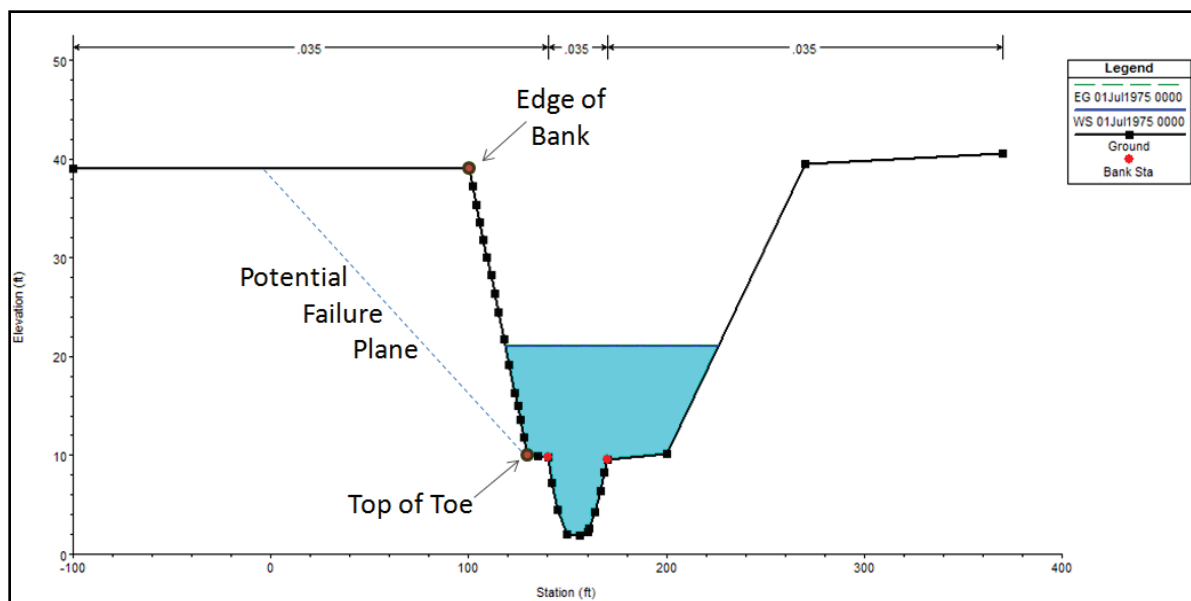


Figure 28. Reasonable location for **Edge of Bank** and **Top of Toe** definitions on an HEC-RAS cross section.

Right Bank Edge Station: Analogous to the **Left Bank Edge** station, the **Right Bank Edge Station** should be the inflection point between the bank and the top of the bank on the left side of the cross section. All failure planes considered will intersect the top of bank between the edge of bank and the last cross section station-elevation point

Left Bank Toe Station: BSTEM divides the bank into two sections, the **Bank** and the **Toe** (Figure 29) sections. Conceptually, the toe is material composed of blocks of failed material or engineered toe protection. Therefore, failure planes are only computed through the bank surface *above* the **Top of Toe**. The **Top of Toe** often corresponds to a break in slope or material type but it does not have to (Figure 29). In future versions of BSTEM, users will be able to select a separate material type for the toe but in the first alpha version of BSTEM, the software adopts the material type of the bank or layer associated with the toe. This parameter can be

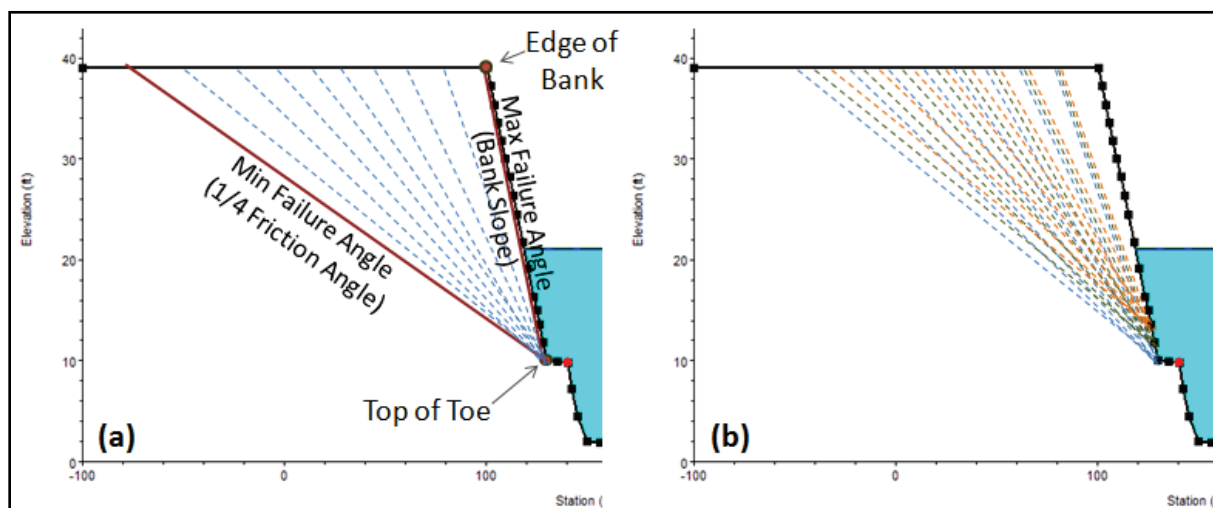


Figure 29. (a) The maximum, minimum and incremental angles evaluated. (b) at each node between the **Top of Toe** and **Edge of Bank**.

automatically set to the HEC-RAS left bank station for every cross section that has **Left Bank Material** defined. From the HEC-RAS **Sediment Data Editor** (Figure 26), click **Set Toe Station to Bank Stations** and click the **Set Toe Stations to Movable Bed Stations** (movable bed limits). Setting movable bed limits and toe stations at the same node is strongly recommended.

Right Bank Toe Station: The **Right Bank Toe** is analogous to the **Left Bank Toe** section and can be set to the right bank station for every bank that has **Right Bank Material** defined. From the HEC-RAS Sediment Data Editor (Figure 26), click **Set Toe Station to Bank Stations** and click the **Set Toe Stations to Movable Bed Stations** (movable bed limits). Setting movable bed limits and toe stations at the same node is strongly recommended.

GW Elev: In order to compute bank failure on either side of any cross section a **Groundwater Elevation** must be specified. Results will be very sensitive to this parameter. BSTEM does not yet have a physical limit to negative pore water pressure so a very low groundwater table could generate nearly infinite bank stability.

*Note: The **Edge of Bank** station defines the range of failure planes as shown in Figure 28. The **Edge of Bank** stations limit the maximum distance of toe scour in the absence of bank failures. Bank failure events move the **Edge of Bank** out from the channel, recognizing a new edge at the top of the failure plane. However, if the BSTEM does not compute bank failures, and toe-scour is primarily responsible for lateral migration, the **Edge of Bank** will not migrate as the bank erodes, and can artificially limit scour, generating near vertical banks at the edge station. In a toe scour-driven model, the edge of bank should be specified far enough to allow the maximum reasonable toe scour.*

If the static groundwater option is selected, BSTEM will use this groundwater elevation for the entire cross section simulation. If the dynamic groundwater option is selected, the user specified groundwater elevation will become the initial elevation, and groundwater will rise and fall in response to changes in channel stage. The overbank is modeled as a "linear reservoir" with a volume determined by the distance between cross sections and the user specified "Reservoir Width" parameter, and is moved between the groundwater reservoir and the channel at the rate of the user specified saturated hydraulic conductivity. The reservoir width and hydraulic conductivity are properties of the cross section material (next section).

UM.3 Defining Cross Section Materials

To define cross section materials for BSTEM, the user will enter information from the HEC-RAS **Sediment Data Editor** (Figure 26) from the BSTEM tab:

Left or Right Bank Material: HEC-RAS requires at least one set of material properties to be specified for each bank it performs bank failure analysis on. Three levels of detail are available for specifying this parameter including:

- a. Selecting Pre-Defined Default Parameters
- b. Select a Single Set of User Defined Material Parameters for a Bank
- c. Define Layers of Unique Material at a Bank

The material specification approach is bank-specific, so different approaches can be used for different banks within the same model.

1. Selecting Pre-Defined Default Parameters

The standalone version of BSTEM includes sixteen default material types that are also included in HEC-RAS. These default material types are each populated with characteristic soil properties distilled from a database of field data collected by the USDA-ARS. The unit weight, friction angle (ϕ'), cohesion, ϕ^b , critical shear stress (τ_c), and erodibility are listed in Table 2. (See the description of these parameters in *Soil Strength Parameters*.)

Table 2. Default materials and material parameters

Default Material Type	Saturated Unit Weight (lb/ft ³)	Friction Angle (ϕ')	Cohesion (lb/ft ²)	ϕ^b	Critical Shear (lb/ft ²)	Erodibility (ft ³ /lb-s)
Boulders	127.3	42.0	0	15	10.4	2.85E-05
Cobbles	127.3	42.0	0	15	2.59	5.73E-05
Gravel	127.3	36.0	0	15	0.23	1.92E-04
Coarse Angular Sand	117.8	32.3	8.354	15	0.0106	8.95E-04
Course Round Sand	117.8	28.3	8.354	15	0.0106	8.95E-04
Fine Angular Sand	117.8	32.3	8.354	15	0.00267	8.95E-04
Fine Round Sand	117.8	28.3	8.354	15	0.00267	8.95E-04
Erodible Silt	114.6	26.6	89.81	15	0.00209	2.01E-03
Moderate Silt	114.6	26.6	89.81	15	0.1044	2.86E-04
Resistant Silt	114.6	26.6	89.81	15	1.0443	8.91E-05
Erodible Soft Clay	112.7	26.4	171.26	15	0.00209	2.01E-03
Moderate Soft Clay	112.7	26.4	171.26	15	0.1044	2.86E-04
Resistant Soft Clay	112.7	26.4	171.26	15	1.0443	2.01E-03
Erodible Stiff Clay	112.7	21.1	263.16	15	14.6	2.01E-03
Moderate Stiff Clay	112.7	21.1	263.16	15	0.1044	2.86E-04
Resistant Stiff Clay	112.7	21.1	263.16	15	1.0443	2.01E-03

Note: These parameters are extremely site specific, and the default parameters are central tendencies of very noisy data sets, particularly for cohesive material types. Therefore, default parameters will often generate substantial errors.

Coupling these bank failure algorithms with the mass balance computations in the mobile bed capabilities in HEC-RAS introduced one additional parameter requirement. Any mass that is "failed" into the channel requires a gradation so HEC-RAS can partition it into grain classes for transport. Therefore, idealized gradations were selected for each material type based on their description. These gradations are depicted in Figure 30.

In order to select one of the default material types, from the table on the **Sediment Data Editor, BSTEM Tab** (Figure 26), from the columns labeled **Left Bank Material** or **Right Bank Material** click at the cross section of interest. A list of default material types that are available will appear (Figure 31). Ignore the option "**DEFINE LAYERS**", from the list and select the desired material type and it will associate it with that bank (Figure 31).

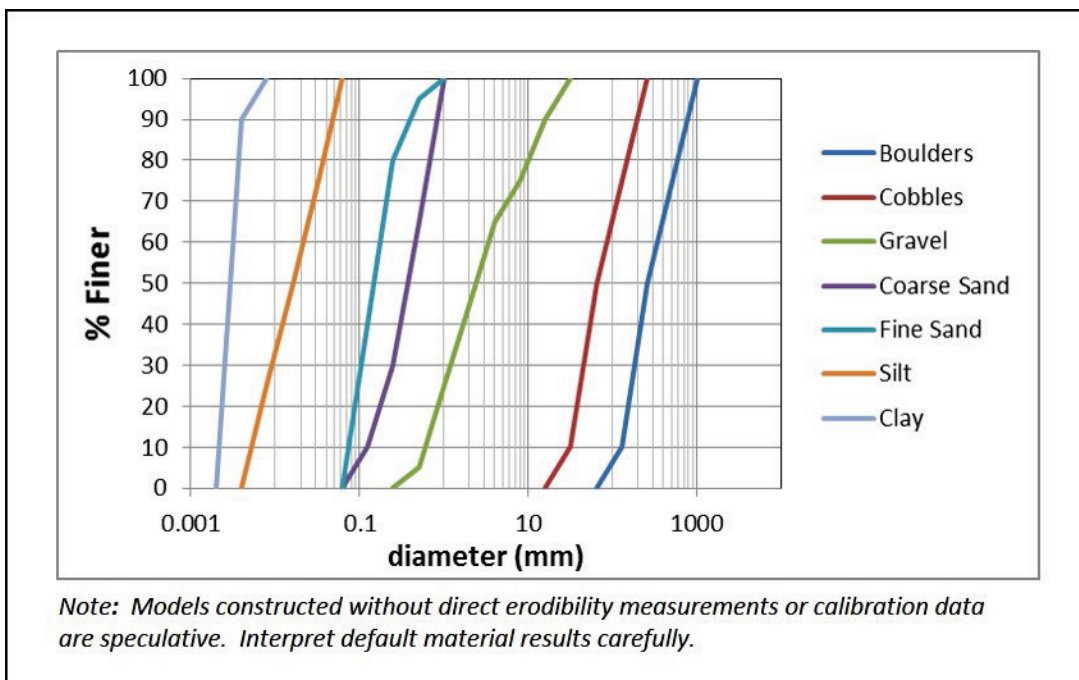


Figure 30. Idealized gradations selected for the default material types.

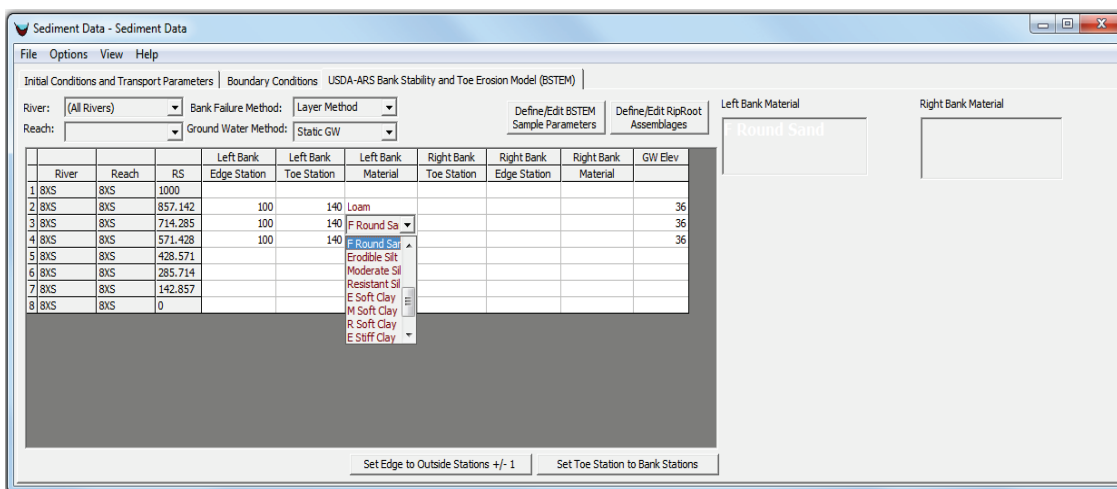


Figure 31. HEC-RAS - Sediment Data Editor - BSTEM Tab - Selecting Cross Section Materials.

2. Select a Single Set of User Defined Material Parameters for a Bank

Because of the inherent variability of these parameters, site specific measurements are recommended. If data is available, customized material types can be associated with a bank. This is analogous to the process for defining sediment gradations in the **Initial Conditions and Transport Parameters Tab** of the **Sediment Data Editor** (Figure 31), where gradation records are defined and then associated with the appropriate cross section.

Before selecting customized materials a user must define the materials by clicking **Define/Edit BSTEM Sample Parameters**. The **BSTEM Material Parameters Editor** will open (Figure 32). To create a new BSTEM material, click **New Record**  and

BSTEM Material Parameters Editor

BSTEM Layer Parameters: Loam

Sat Unit Weight: 120 lbf/ft³

Friction Angle: 23 degrees

Cohesion: 20 lbf/ft²

Phi b: 15 degrees

Gradation Sample: Sand

Critical Shear Stress: 0.001 lbf/ft²

Erodibility: 0.00009 ft³/lbf-s

Estimate Parameters

Ground Water Parameters (Optional)

Sat Hydr Conductivity (K): 0.8 ft/d

Reservoir Width (L): 100 ft

OK Cancel

Figure 32. BSTEM Material Parameters Editor.

specify the name. HEC-RAS will reject any names that are identical to existing or default material names. Five mandatory intrinsic soil strength parameters (used to compute the failure plane and factor of safety), two mandatory erodibility parameters (used to compute toe scour) and one optional parameter can then be entered.

Soil Strength Parameters

The first five parameters are intrinsic soil strength parameters and are associated with the computation of a critical failure plane and the FS associated with that failure plane. These five parameters emerge from classical geotechnical measurements that most soils labs would be able to handle. HEC-RAS uses four user defined parameters with hydrodynamic and geometric data to compute a factor of safety for a range of possible failure planes by computing the ratio of the resisting forces to the driving forces: cohesion (c'), saturated unit weight (W), the angle of internal friction (ϕ'), and the angle representing the relationship between shear matrix suction and apparent cohesion (ϕ^b). These four user defined parameters are entered in the **BSTEM Material Parameters Editor** (Figure 32) and are described below.

Unit Weight: This is the *saturated* unit weight (combined weight of the solids and water of the soil when saturated). Note that this is different than the unit weight used elsewhere in HEC-RAS sediment transport computations. The unit weight used elsewhere in HEC-RAS sediment transport computations is the mass of the solids per unit volume.

Friction Angle (ϕ'): The friction angle is a classic geotechnical parameter that is a measurement of the soil strength that quantifies the friction shear resistance of soil. The "angle" of the "friction angle" is derived from the Mohr-Coulomb failure criterion (Labuz, 2012) and is the angle of inclination in the classical Mohr diagram. The angle of inclination is a theoretical angle (the rate of increasing strength with increasing normal force) used to compute soil strength and should not be confused with physically intuitive angles like the angle of repose. Also, the angle of inclination is not the minimum angle of the failure plane. In cases where groundwater elevation is higher than the water surface elevation the bank can lose frictional strength and be left only with cohesion, allowing for a shallower failure plane angle. The friction angle can be determined by collecting "undisturbed" cores for tri-axial testing in a soils laboratory or it can be measured *in situ* with a borehole shear test. The Iowa Borehole Shear device (Thorne, 1981) is a hand held instrument that is commonly used to collect this parameter from hand augured eight centimeter boreholes for BSTEM studies.

Cohesion: Cohesion is the attractive force of particles in a soil mixture, usually as a result of electrochemical or biological bonding forces. These forces increase the strength of a soil matrix. Cohesion is generally a minor consideration in granular soils but can account for a substantial amount of soil strength in cohesive materials. Cohesion is computed from the same data as the friction angle and, therefore, must be measured either by tri-axial laboratory tests or *in situ* borehole shear measurements.

Phi b (ϕ^b): As soil drains, capillary tension induce negative pore water pressure or matrix suction. Suction resists bank failure and increases the shear strength of the soil matrix. In the bank failure algorithms, suction is quantified as an "apparent cohesion" or the equivalent increase in cohesion required to generate the same increase in shear strength (Figure 33). ϕ^b is a function of soil moisture and maximizes at the friction angle (ϕ') at saturation. For most materials ϕ^b is generally between ten to thirty degrees

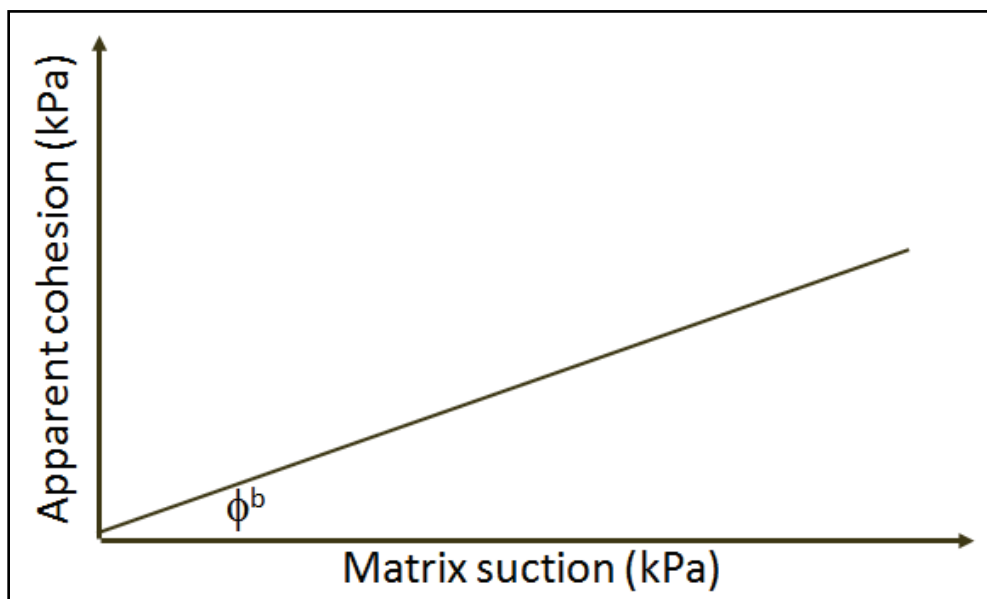


Figure 33. ϕ^b is the slope of the relationship between matrix suction and apparent cohesion.

depending on soil type. ϕ^b is very difficult to go out and fundamentally measure ϕ^b . ϕ^b has been measured a handful of times in research settings. Most applications start between ten and fifteen degrees but ϕ^b goes to a maximum of the friction angle when the material is saturated (Fredlund, 1996). Because of the estimated nature of this parameter it can be used as a calibration factor.

Gradation Sample: HEC-RAS requires a fifth bank material parameter that is required but not used until after the failure calculation. In order to partition any failed material into grain classes for transport by the sediment transport model, the bank material has to have a bed gradation associated with it. Bed gradations are defined by clicking **Define/Edit Bed Gradation** from the **Initial Conditions and Transport Parameters** Tab of the **HEC-RAS Sediment Data Editor** (Figure 34).

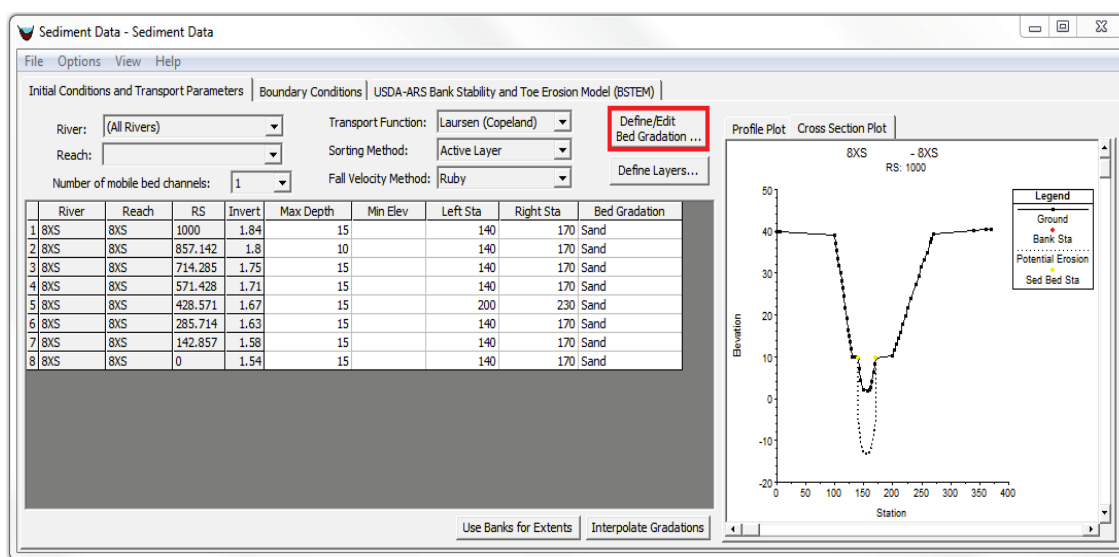


Figure 34. Defining bed gradations.

Any gradations defined here become automatically available in the **Gradation Sample** list on the **BSTEM Material Parameter Editor** (Figure 32).

Erodibility Parameters

The second set of parameters on the **BSTEM Material Parameters Editor** (Figure 32) are the erodibility parameters. These parameters are specialized for bank failure analysis. Erodibility parameters are measurements of the erodibility of the soils in response to hydrodynamic forcing. Standard soil testing laboratories are not likely to have the capabilities to collect these parameters. However, the USACE Coastal and Hydraulic Lab (ERDC-CHL), other federal agencies, and several universities can quantify these parameters. Bank jet tests (Hanson, 2001) and Sedflume laboratory tests (Borrowman, 2006) are the best ways to estimate these parameters.

Critical Shear Stress: Critical shear stress is when the bank begins to scour.

Erodibility: The rate of sediment removal in response to a unit shear stress.

In the absence of these parameters, Casagli (1999) described a relation between critical shear stress and erosion of the cohesive and non-cohesive banks based on the shear stress relations of Komar (1987) and Millar (1993). Additionally, Simon (2000) summarized their database of *cohesionless* measurements to find a relationship between critical shear stress and erodibility:

$$E = 1.42\tau_c^{-0.824}$$

This relationship is based on the regression depicted in Figure 35 which includes a great deal of scatter in log space. This underscores the variable and site specific nature of these parameters, therefore local measurement of these parameters is highly recommended. Also note that this relationship does not account for cohesion and, therefore, should not be used for cohesive soils.

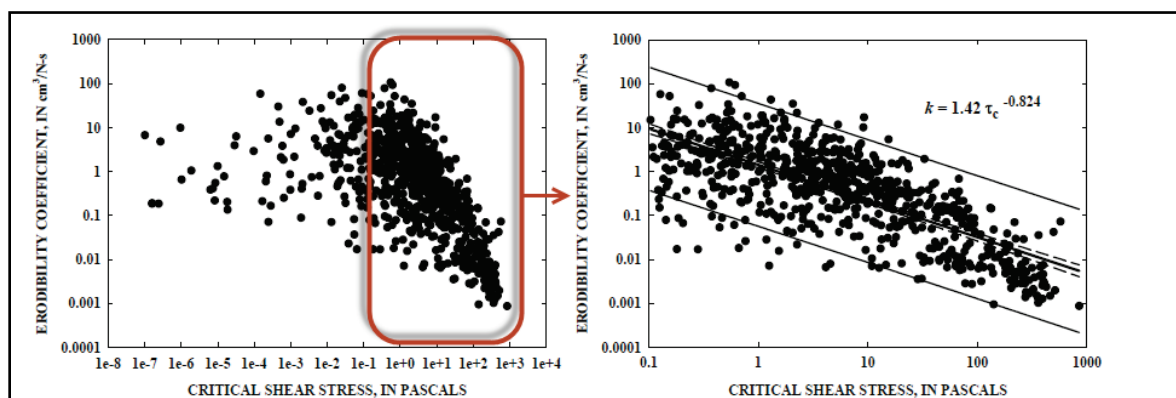


Figure 35. Relationship between erodibility and critical shear stress from Simon et al. (2000).

Groundwater Parameters (Optional)

Groundwater parameters are optional and are only used if the dynamic groundwater option is selected in the HEC-RAS BSTEM interface. There are two parameters that determine the rate that water can drain from or infiltrate into a bank. In turn, this determines the lag between the rising or falling of groundwater elevation with respect to the water surface elevation.

Hydraulic Conductivity: The hydraulic conductivity for this model is the standard Darcy "K" parameter used in groundwater modeling. The hydraulic conductivity is a linear parameter that determines velocity of groundwater proportional to a gradient. Hydraulic conductivity can be measured with field or laboratory tests but is also often documented in regional literature or estimated by expert intuition (analogous to Manning's n).

Reservoir Length: Groundwater dynamics follows a simple linear reservoir model that assumes the banks store water. Water can be added to or drained from the rate of the saturated hydraulic conductivity. The "length" of this reservoir is the bank thickness (perpendicular to the river) that contributes water to the river on pertinent time scales.

If the soils are very permeable or the reservoir is small (high K or low L) the groundwater elevation will track the channel water surface elevation (Figure 36a). If the soils are impermeable or the reservoir is very large, the groundwater will not respond much to flow depth in the channel (Figure 36b). However, intermediate hydraulic conductivities will introduce a lag between channel water surfaces and

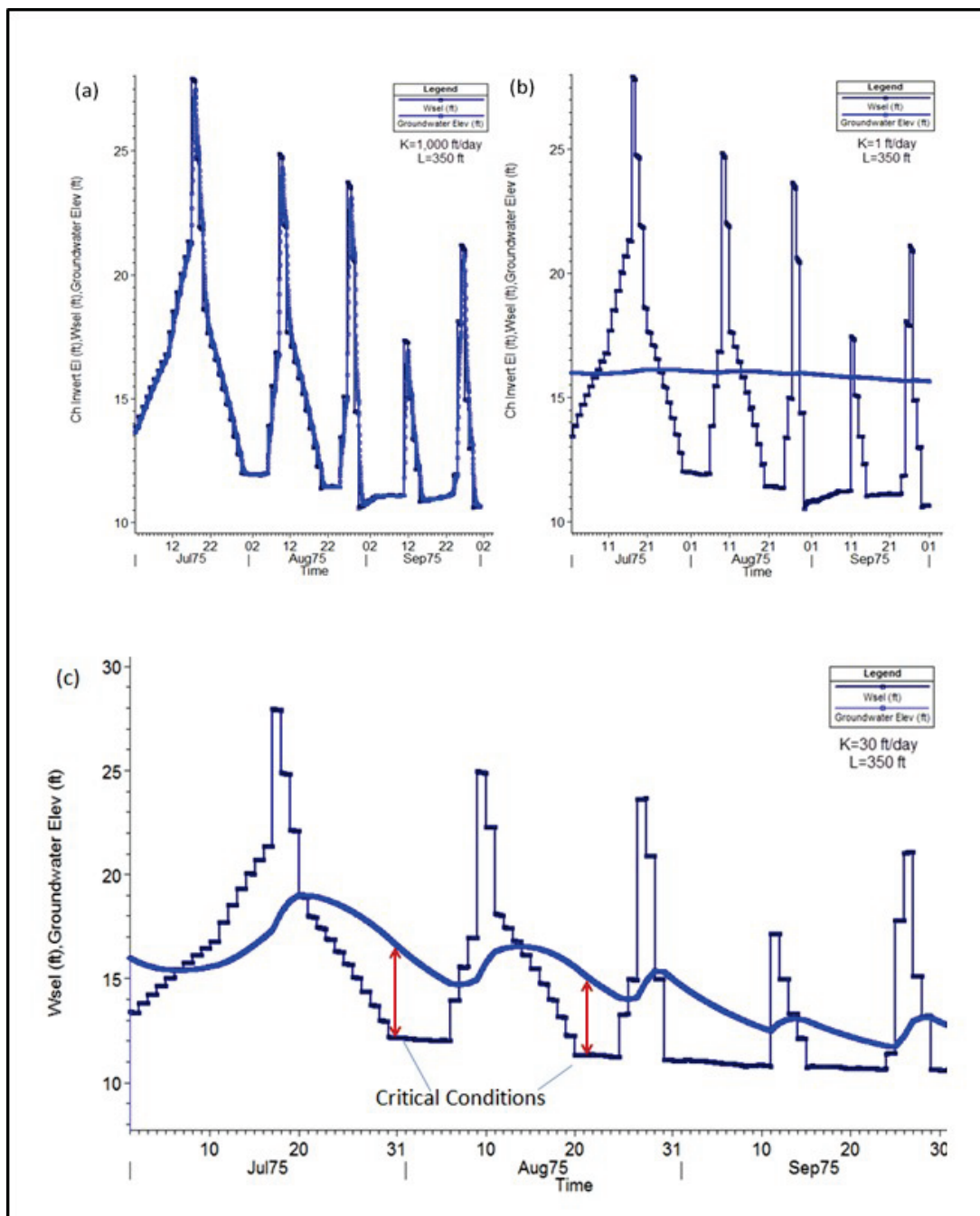


Figure 36. Groundwater response to (a) high (b) low and (c) moderate hydraulic conductivities.

groundwater elevation (Figure 36c). Because groundwater elevations higher than the confining water surface elevation are the critical condition, groundwater lag can induce failures on the falling limb of the hydrograph, both in the field and in the model.

3. Define Separate Parameters for Multiple Layers for Each Cross Sections

Finally, it is often advantageous to define several bank material layers. Some banks have distinct stratigraphy, stacking soil layers. Sometimes vegetation is modeled by introducing a surface layer with the same friction angle as the parent material but with a higher cohesion. To specify layers, select **Define Layers**, from the **Left/Right Bank Material** lists available in the **HEC-RAS Sediment Data Editor** (Figure 37). If the **Define Layers** option is selected, a new table will appear on the right side of the editor (Figure 37).

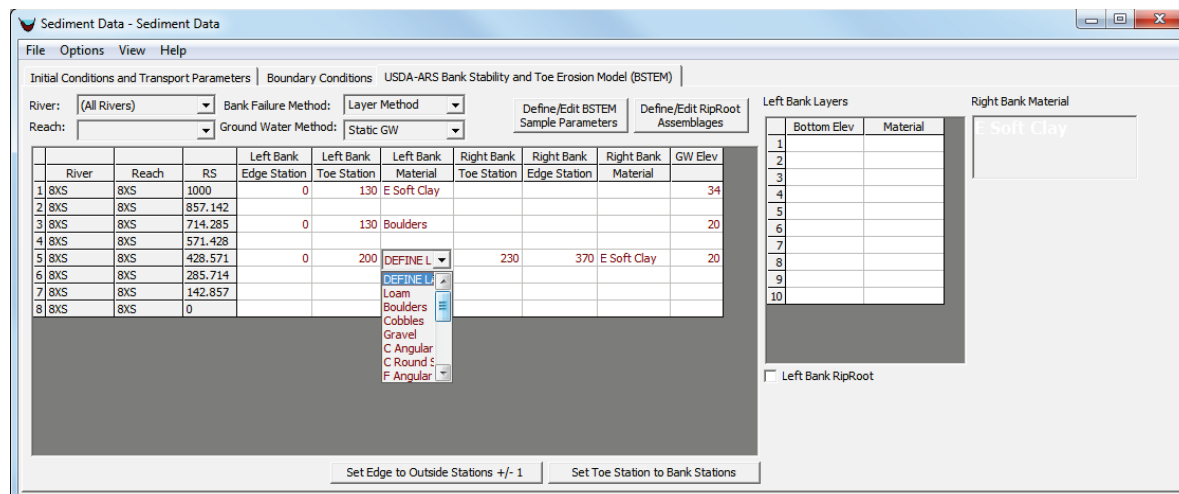


Figure 37. Selecting the layer mode for a bank failure.

The bank material layer table requires two parameters: a bottom elevation and a material. Layers must be ordered from top to bottom, i.e., the upmost layer in the first row, the next lowest layer in the second row, etc. The first layer will extend from the highest point on the half-cross section to the specified **Bottom Elevation**. Subsequent layers will use the bottom elevation of the preceding layer as an upper boundary. Add layers until the lowest layer's **Bottom Elevation** extends below the conceivable bottom of the model (i.e., the lowest elevation the model is likely to scour to). The bottom of the deepest layer has to at least extend to the thalweg elevation for the model to run. Then, just like the **Bank Material Type** option in the main BSTEM editor, a list of bank materials can be accessed by clicking on the **Material** column (Figure 38). Each layer has to have its own material specified, but the materials do not have to be unique and can be any combination of default or user specified material types.

Guidelines for Selecting Layer Elevations: Setting layer elevations according to a couple conventions can make an HEC-RAS/BSTEM model more stable. First, set the bottom of the top layer below the lowest point of the overbank, so the layer only intersects the cross section at one point, between the toe and the top of bank (Figure 39). Second, set the bottom of the bottom layer below the deepest possible thalweg elevation (e.g., thalweg max erodible depth) so the model never scours below the defined layers (Figure 39).

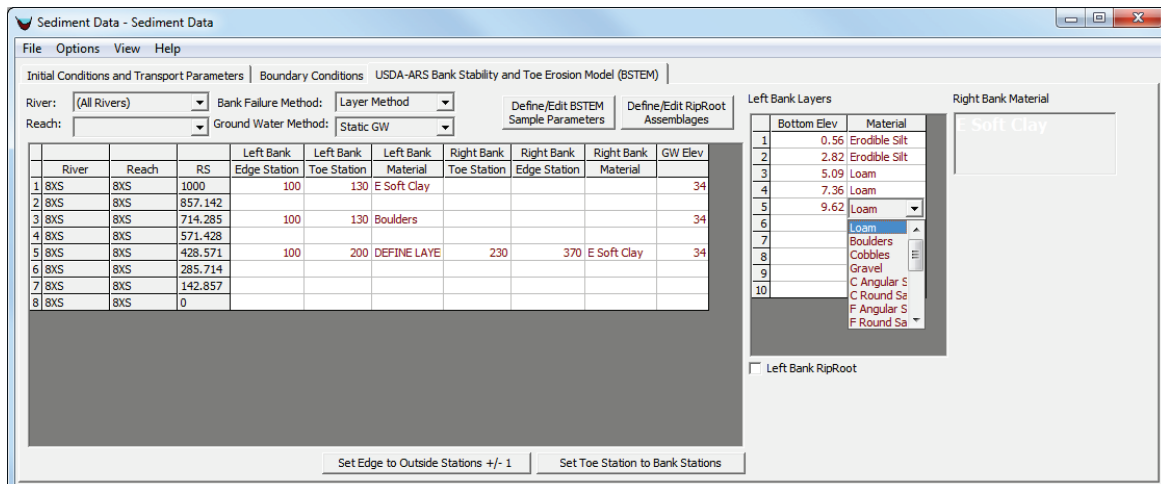


Figure 38. Defining layers and layer material types.

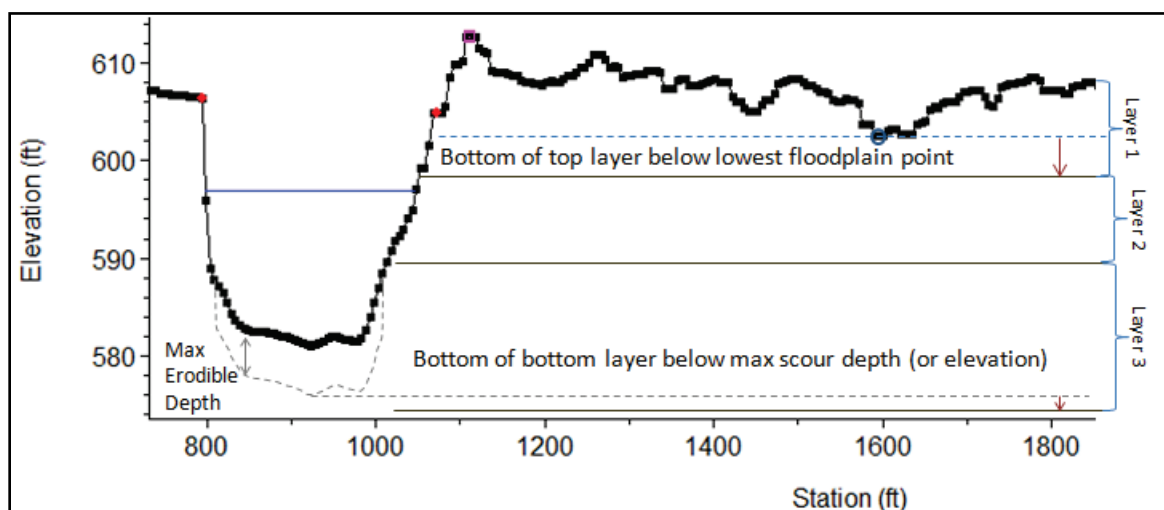


Figure 39. Guidelines for setting layer elevations.

UM.4 USDA-ARS BSTEM Options

The HEC-RAS/BSTEM model integration includes several arbitrary parameter thresholds and two processes with multiple methods. These parameters and methods influence results and run times. The **BSTEM Options Editor** (Figure 40) exposes them so users can adjust or select them.

UM.4.1 Number of Failure Plane Computation Nodes

The bank failure algorithm computes a critical failure plane at every one percent of the elevation between the toe and edge stations, computing critical failure planes at 100 evenly spaced vertical bank intersection points (Figure 13). This is computationally expensive and often much more detail than necessary. From HEC-RAS this parameter is available from the **BSTEM Options Editor** (Figure 40). Users can specify the number of vertical computation bank failure points. HEC-RAS will evenly distribute the computation points vertically, between the bank toe and edge elevations.

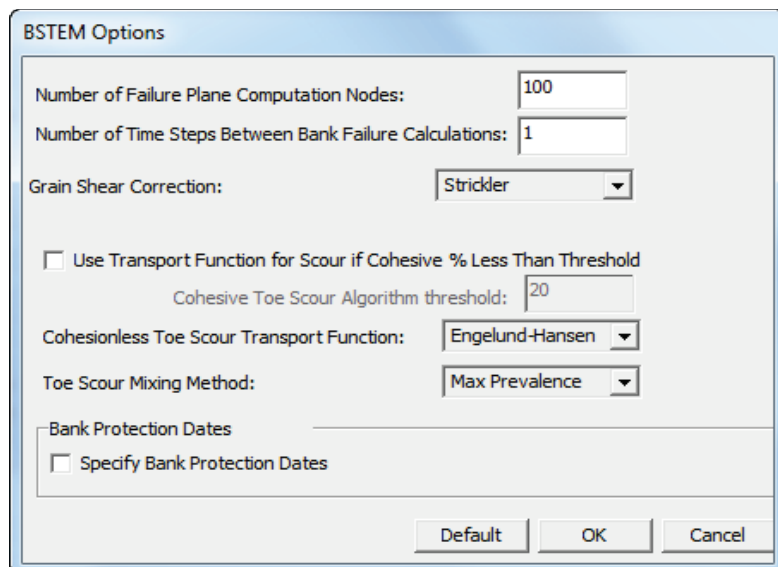


Figure 40. BSTEM Options Editor.

UM.4.2 Number of Time Steps between Failure Computations

Bank failure algorithms are computationally expensive. These algorithms can increase sediment model run times by an order of magnitude. Users can reduce run times by defining BSTEM parameters only at the half-cross sections where bank processes are expected. Bank failure conditions (i.e., FS less than one) are not usually instantaneous. If FS drops below one, the failure condition generally lasts for several time steps. Skipping bank failure computations will introduce error, but given the uncertainties of the model, the error may be acceptable tradeoff for run time.

UM.4.3 Grain Shear Correction

Only part of the shear stress water exerts on soils translates into transport. Shear partitioning theory for bed transport is more mature, parsing shear into form and grain shear (and sometimes into other components). This theory is not as applicable to banks. However, the isolated measurements, either by jet tests in the field or Sedflume in the lab, tend to isolate grain shear effects. Therefore, the toe scour mechanisms apply a **Strickler** grain shear correction by default. From the **BSTEM Options Editor** (Figure 40), from the **Grain Shear Correction** list, select **None**, this will turn the correction off. Turning the grain shear correction off will increase the shear stress on the bank and will increase scour.

UM.4.4 Minimum Percent Cohesive to Use Toe Scour Algorithms

BSTEM has two approaches to toe scour. The cohesive algorithms use the excess shear equation to compute scour rates based on measured erodibility data. The cohesionless algorithms apply transport functions (Section UM.4.5) to compute scour. The cohesionless methods are generally less accurate, but it is difficult to estimate cohesionless erodibility either in the lab or in the field.

By default, HEC-RAS/BSTEM uses the cohesionless methods. The **Use Transport Methods** check box in the **BSTEM Options Editor** (Figure 40), is off by default, forcing HEC-RAS to use the cohesionless, excess shear method. Applying the transport functions to individual nodes often wildly over predicts transport and scour, so users must intentionally turn the cohesionless methods on by checking the **Use Transport Methods for Scour if Cohesive % is Less than Threshold** feature.

If cohesionless methods are selected, HEC-RAS/BSTEM decides between the methods for each soil layer by computing the percentage of the bank soil that is cohesive (i.e., in the first five HEC-RAS grain classes, which is less than .063 millimeters in the default grain class definition). HEC-RAS computes this percentage from the gradation defined in the sediment editor and selected in the **BSTEM Material Parameter Editor** (Figure 32) from the soil type list, or the narrow gradations of the default soil types (Figure 30). By default, if **20 percent** or more of the soil is cohesive, (clay or silt), BSTEM uses the cohesive methods, applying cohesionless equations if the cohesive fraction is less than **20 percent**.

The twenty percent threshold is not entirely arbitrary. Around twenty percent cohesive content, the fine particles fill the soil voids enough for their cohesive properties to dominate the erodibility of the larger particles. However, in reality, the transition from cohesive matrix support to cohesionless framework support is a gradient not a step function. Therefore, the cohesive percentage threshold is exposed as an option in the **BSTEM Options Editor** (Figure 40). If the transport functions return unreasonable scour rates, as often happens, users can model cohesionless materials with the cohesive erodibility approach.

UM.4.5 Transport Function

As described in Section UM.4.4, if a soil layer has less than 20 percent (or a user specified percentage) cohesive material, BSTEM will apply a transport function to compute toe scour (Figure 41). The USDA-ARS BSTEM model uses an NCED (National Center for Earth Surface Dynamics) transport function library to compute transport. This library includes six transport functions, including:

- Englund-Hansen (1967)
- Parker (1990)
- Wilcock and Crowe (2000)
- Meyer-Peter Muler
- Wu (2000)

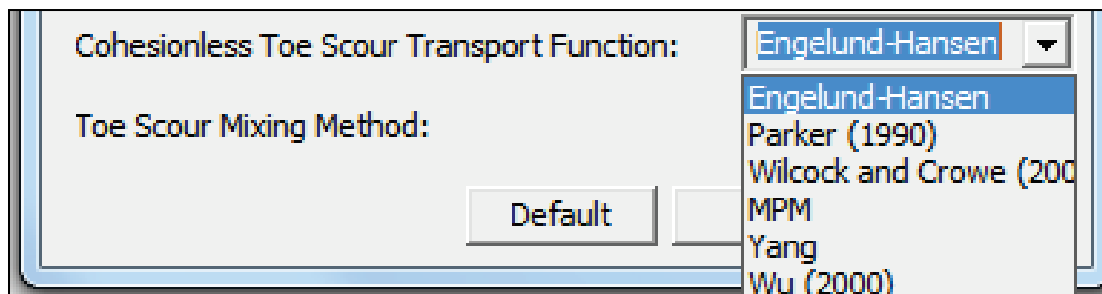


Figure 41. BSTEM Options Editor - Transport functions available for cohesionless toe scour in BSTEM.

Select and apply transport functions with *extreme caution* recognizing the intent and range of applicability of each. Transport functions are notoriously uncertain, computing transports that commonly differ by at least one order of magnitude. The Engelund-Hansen (1967) and Yang (1973) transport equations work best for sand. The Meyer-Peter-Mueller (MPM) transport function will probably perform best for coarse materials. Parker (1990) and Wilcock and Crowe (2003) are both **surface-based** methods, intended for heterogeneous soil mixtures with sand and gravel components. These two methods account for mixing, hiding and armoring implicitly, which tends to moderate transport and sometimes makes the methods more appropriate for toe scour in heterogeneous materials.

Also, it should be noted that most of these transport functions were derived for one-dimensional alluvial transport at the cross section scale. BSTEM applies these transport functions to bank scour at the node scale. This makes transport functions, already uncertain in their intended setting, loose process analogies in toe scour. The transport functions often over predict scour substantially and results should be interpreted carefully.

UM.4.6 Toe Scour Mixing Method

The HEC-RAS sediment transport follows HEC-6 and most sediment transport models by apportioning transport across available grain classes in proportion to the gradation of the bed.

$$T_c = \sum_{j=1}^n \beta_j T_j$$

Where T_c is the total transport capacity, n is the number of grain size classes, β_j is the fraction of material in grain size class j , and T_j is the transport potential computed for material in grain class j . This approach generally works when coupled with an "active layer" bed model that tracks the gradation of a surface layer separately. Without an active layer, transport functions compute huge masses for small particles, removing these materials from deep within the bed, much deeper than physically possible.

The toe scour method does not have an active layer. Therefore, transport methods have unrestricted access to all the fine materials in the bank. Apart from the standard uncertainty of the transport functions, this is the primary reason that the cohesionless method over predicts transport; it can numerically wick fine materials deep in the bank, while the coarser materials remain.

The HEC-RAS/BSTEM development team experimented with three mixing methods to mitigate this numerical artifact:

Cumulative: Applies the same assumption as the bed, apportioning capacity by the prevalence in the bank layer. However, since the bank layer has no active layer and does not update, this provides an unlimited supply of finer material and usually over-predicts scour.

Maximum Prevalence (default): This method apportions capacity according to the relative proportion of the bank gradation. However, it only erodes the most prevalent grain class.

This assumes that the dominant grain class moderates scour. This method is more appropriate if trace fines and low percentage fine sands cause the other methods to over-predict scour and was designed for framework supported materials.

Maximum Capacity: This method was designed for matrix supported materials. It assumes that the prevalent fine material, the one with the largest product of transport potential and prevalence, controls the scour distance. So the scour distance associated with the largest capacity grain class is applied, assuming that the other particles are larger clasts that will fall into the channel when released from the scoured fine matrix.

UM.5 Output

HEC-RAS does not compute USDA-ARS BSTEM results by default. BSTEM output can be selected from the **Sediment Transport Analysis** dialog box, from the **Options** menu, click **Sediment Output Options**. The **Sediment Output Options** dialog box will open. From the **Output Level** list box select **6**. After running the model, go to the **View** menu of the HEC-RAS main window (Figure 25) and select **Sediment Output**. The **Sediment Plot** viewer will open. In general, the new sediment output (which reads HDF5 output), is more complete and user friendly. However, the legacy sediment output viewers from HEC-RAS Version 4.1 were retained because they have a few capabilities (e.g., plotting multiple variables and creating new geometry files) that the new viewers lack.

HEC-RAS computes several commonly used BSTEM results for display in the **Sediment Output** interface. The total mass eroded from a cross section in a computation increment (for both banks and both processes) is reported under **BSTEM All**. The total mass eroded from the banks can also be reported by grain class (e.g. BSTEM (7)) or by bank and process (Figure 42). Finally, FS for each bank (Figure 43) and **Groundwater Elevation** (Figure 44) are available. All of these variables can be viewed as profiles (all the cross sections in a reach at a selected time step) or as time series, (all values over time at a selected cross section). The BSTEM output variables are defined in Table 3.

HEC-RAS modifies cross sections when the sediment model computes bed change or when BSTEM computes bank migration. Viewing cross section changes is often the most valuable output to understand and troubleshoot an HEC-RAS/BSTEM model. Cross section output files can be very large. HEC-RAS only outputs starting and final cross sections by default. The user can request more frequent cross section output from the **Sediment Output Options** dialog box (Figure 45). From the **Sediment Transport Analysis** dialog box, from the **Options** menu, click **Sediment Output Options**. The **Sediment Output Options** dialog box will open (Figure 45), users can request cross section data and specify the increment, an example is provided in Figure 46. The new **Sediment Output Viewer** also plots the water surface elevation and the BSTEM toe associated with the cross section (Figure 47).

UM.6 Model Validation

Model testing was conducted to demonstrate the reliability of the HEC-RAS/BSTEM algorithms. Several test scenarios were constructed and modeled with HEC-RAS, the standalone version of BSTEM 5.4 and the standalone FORTRAN version of BSTEM used in the integration (which

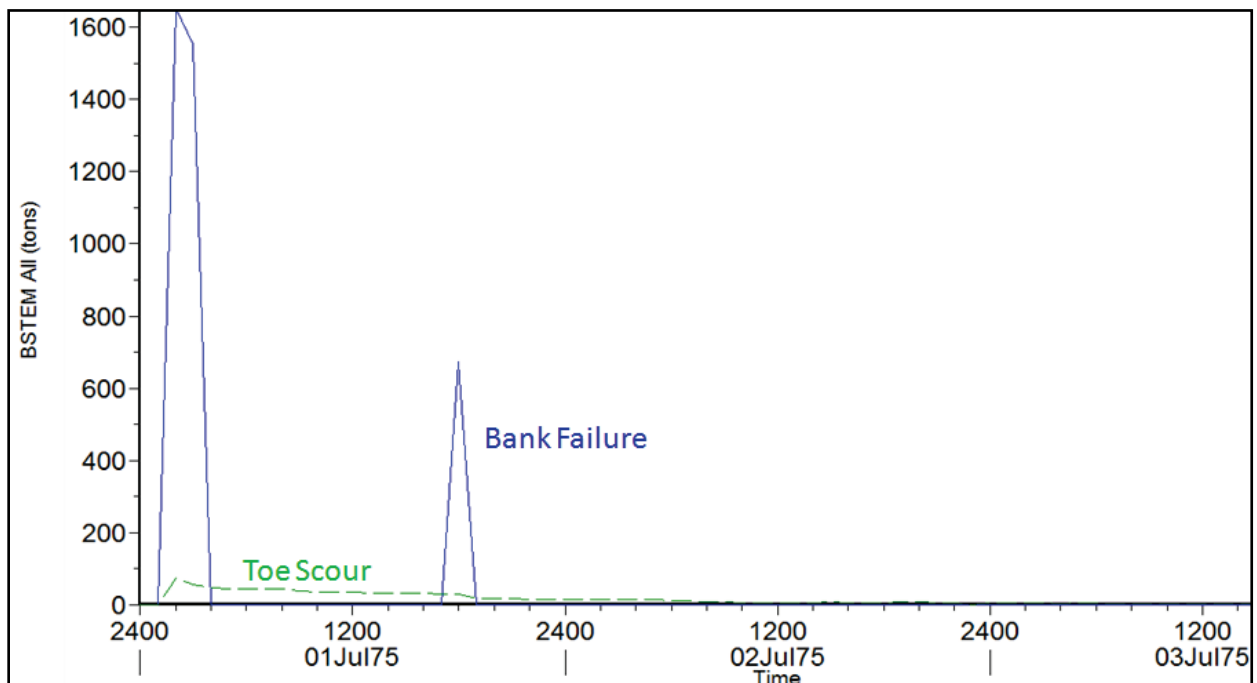


Figure 42. Time series of bank mass eroded by process.

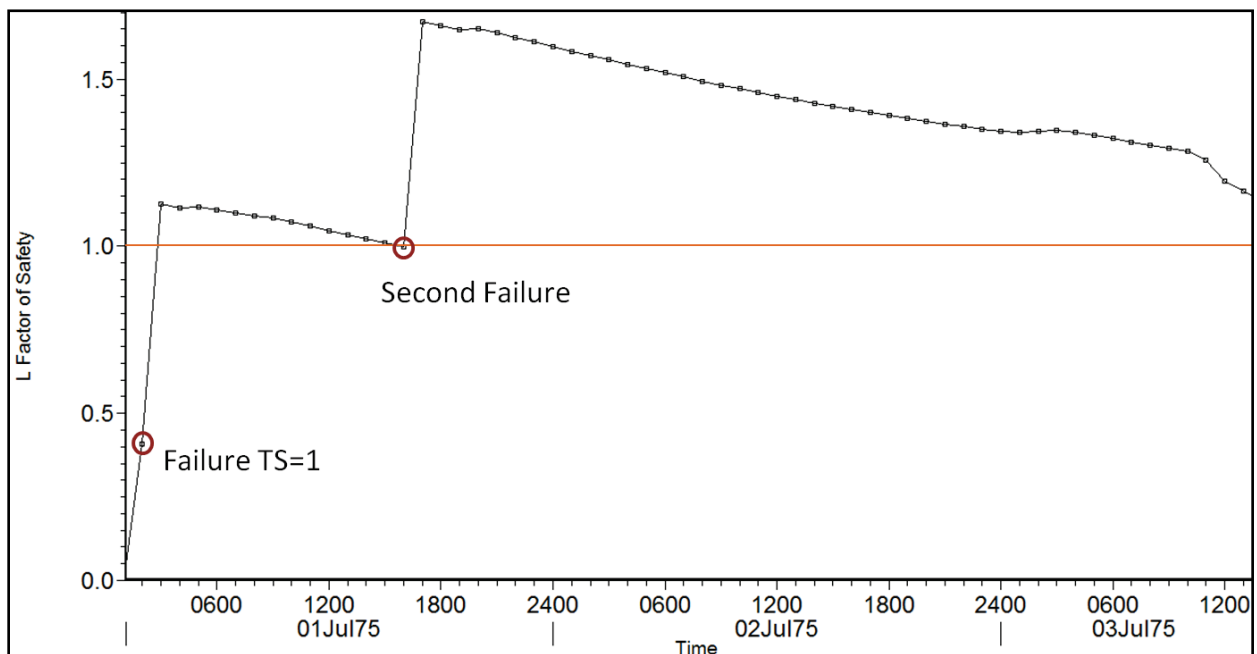


Figure 43. Time series of FS.

was subjected to rigorous independent validation against BSTEM 5.4 (Simon, 2010)). The before and after cross sections for a bank failure event are displayed in Figure 48. The FORTRAN version of the algorithms in HEC-RAS replicates BSTEM 5.4 very closely. Small divergence can be explained by a couple of algorithm differences between the FORTRAN version and BSTEM 5.4.

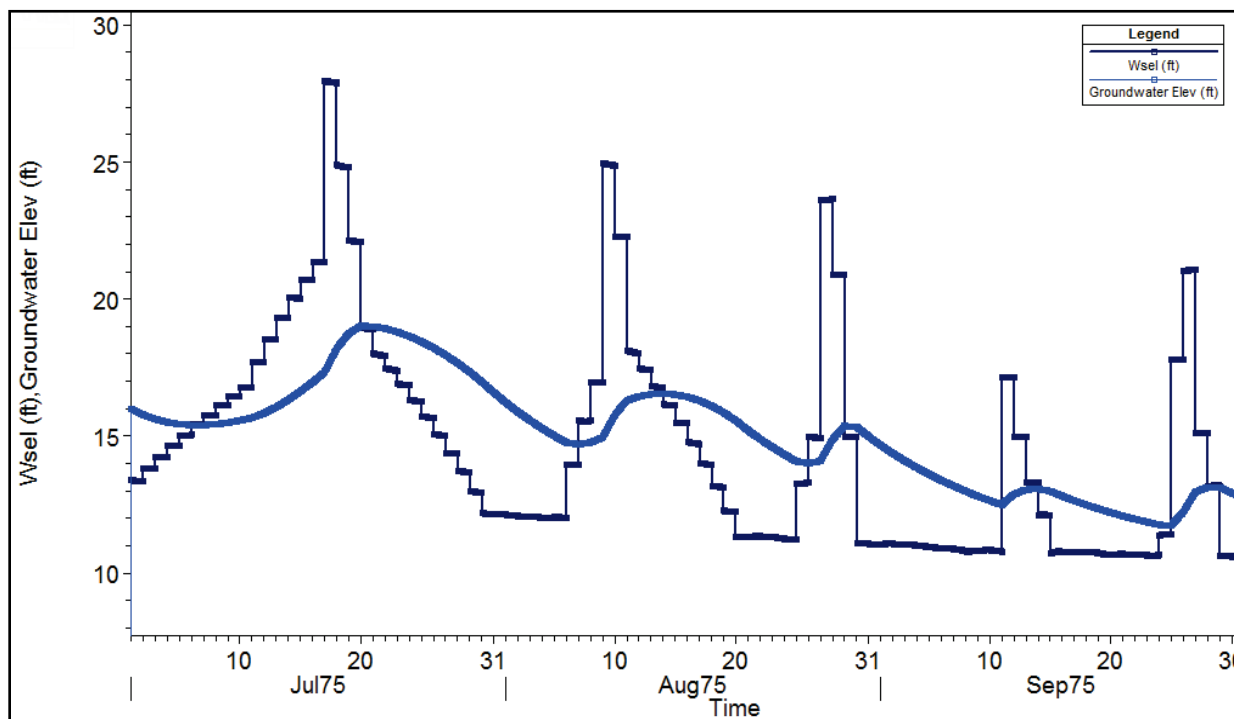


Figure 44. Groundwater and water surface time series plot demonstrating the lag between water surface and groundwater elevations.

Table 3. USDA-ARS BSTEM Output Variables in HEC-RAS.

Variable	Descriptions
BSTEM All (tons or cubic feet)	Total sediment mass (or volume) removed by both banks by toe scour and bank failure for each cross section for each computation increment.
BSTEM (for every grain class) (tons or cubic feet)	The previous variable, subdivided by grain class.
L BSTEM Mass Failure (tons or cubic feet)	Mass removed from the left bank by failure processes for each computation increment.
L BSTEM Mass Toe (tons or cubic feet)	Mass removed from the left bank by toe scour for each computation increment.
L Factor of Safety (Decimal Fraction)	Minimum factor of safety computed in the left bank for each computation increment.
R BSTEM Mass Failure (tons or cubic feet)	Mass removed from the right bank by failure processes for each computation increment.
R BSTEM Mass Toe (tons or cubic feet)	Mass removed from the right bank by toe scour for each computation increment.
R Factor of Safety (Decimal Fraction)	Minimum factor of safety computed in the right bank for each computation increment.
Groundwater Elev (feet)	Groundwater elevation computed in BSTEM, either static, user specified, or computed with the groundwater lag method.

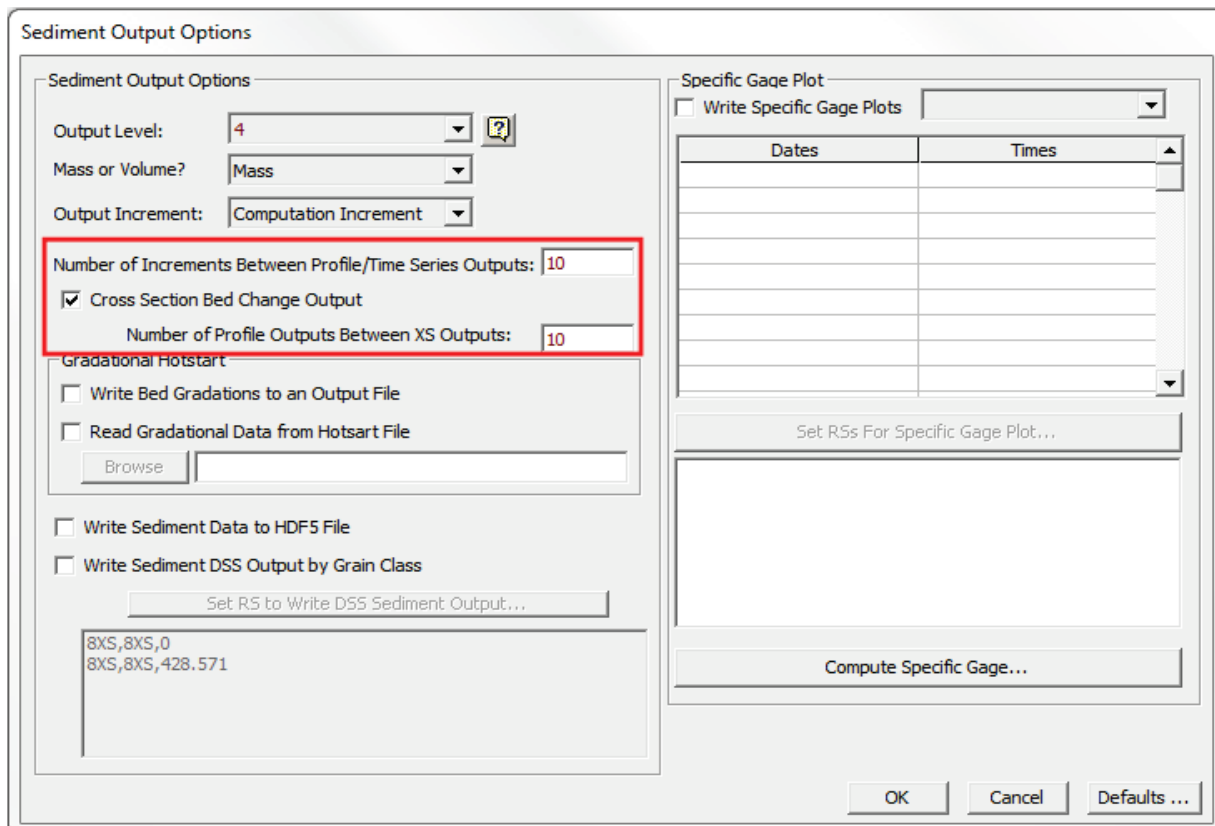


Figure 45. Requesting and specifying the frequency of sediment cross section output in the **Sediment Output Options** dialog box.

Gibson (2015) also applied the model to Goodwin Creek, following the work of Langendoen (2008). Goodwin Creek is a highly instrumented reach with substantial bank migration, carefully measured over a decade with dozens of repeated cross sections, making it an ideal site for evaluating a bank process model. Gibson (2015) used the parameters from Langendoen (2008), to test the model against a known calibration. The integrated HEC-RAS/USDA-ARS BSTEM model performed well compared to prototype data (Figure 49) and the CONCEPTS model runs in Langendoen (2008).

UM.7 Modeling Guidelines, Tips, and Troubleshooting

The HEC-RAS/BSTEM development team has compiled several modeling tips and guidelines that can make coupled bed-bank modeling more stable and less frustrating. Consider the following approaches and tips before setting up a model or to help troubleshoot models that are crashing or behaving poorly.

UM.7.1 Stepwise Modeling Process

Sediment transport modeling with HEC-RAS was already complex and highly parameterized before bank failure. Bank failure makes it more complex. Complex models that account for more processes explicitly make careful, strategic, sequential modeling practice more important.

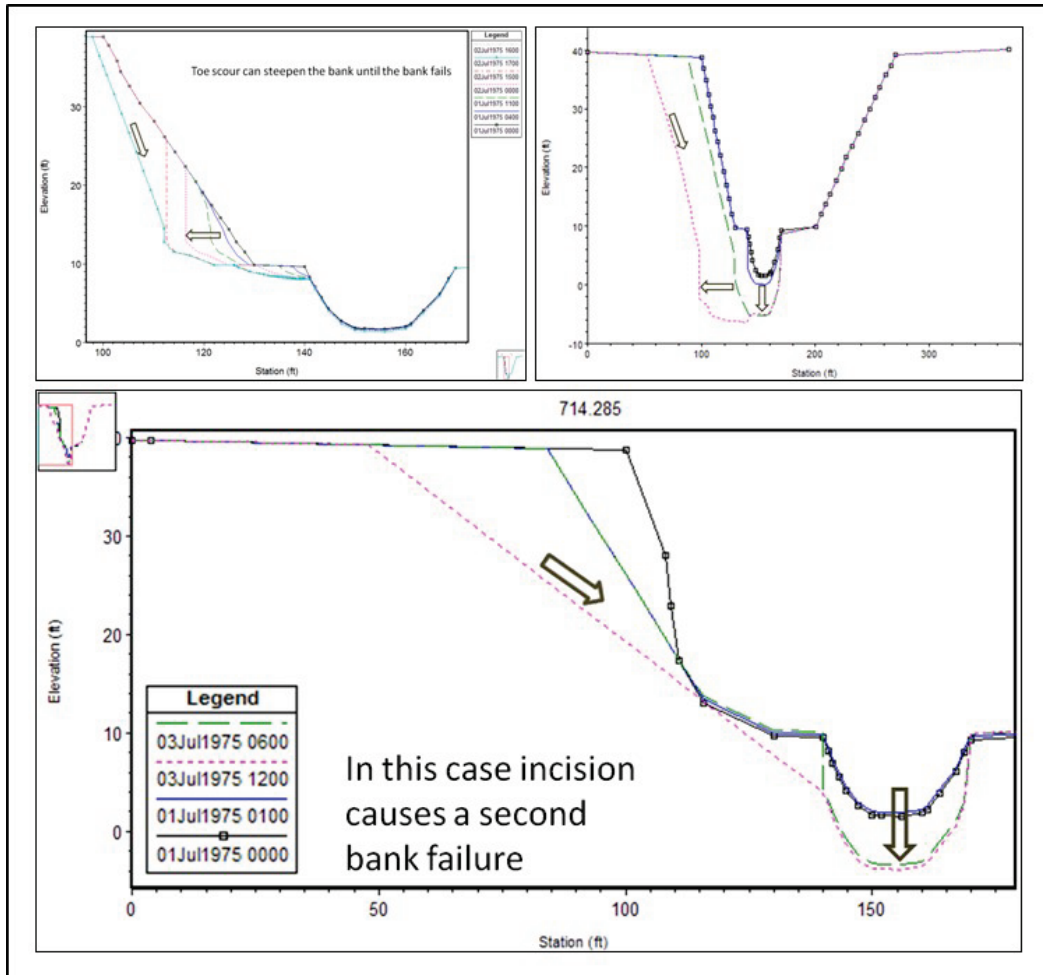


Figure 46. Example HEC-RAS cross section outputs including toe scour, incision and bank failure at various stages in the simulations.

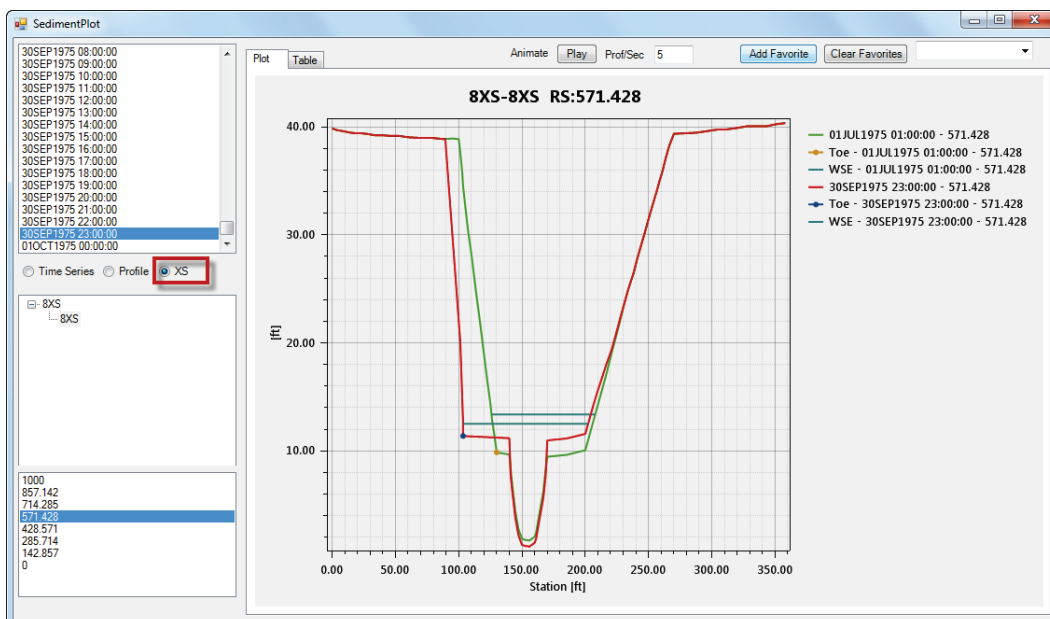


Figure 47. Bank migration cross section output with the new Sediment Output viewer.

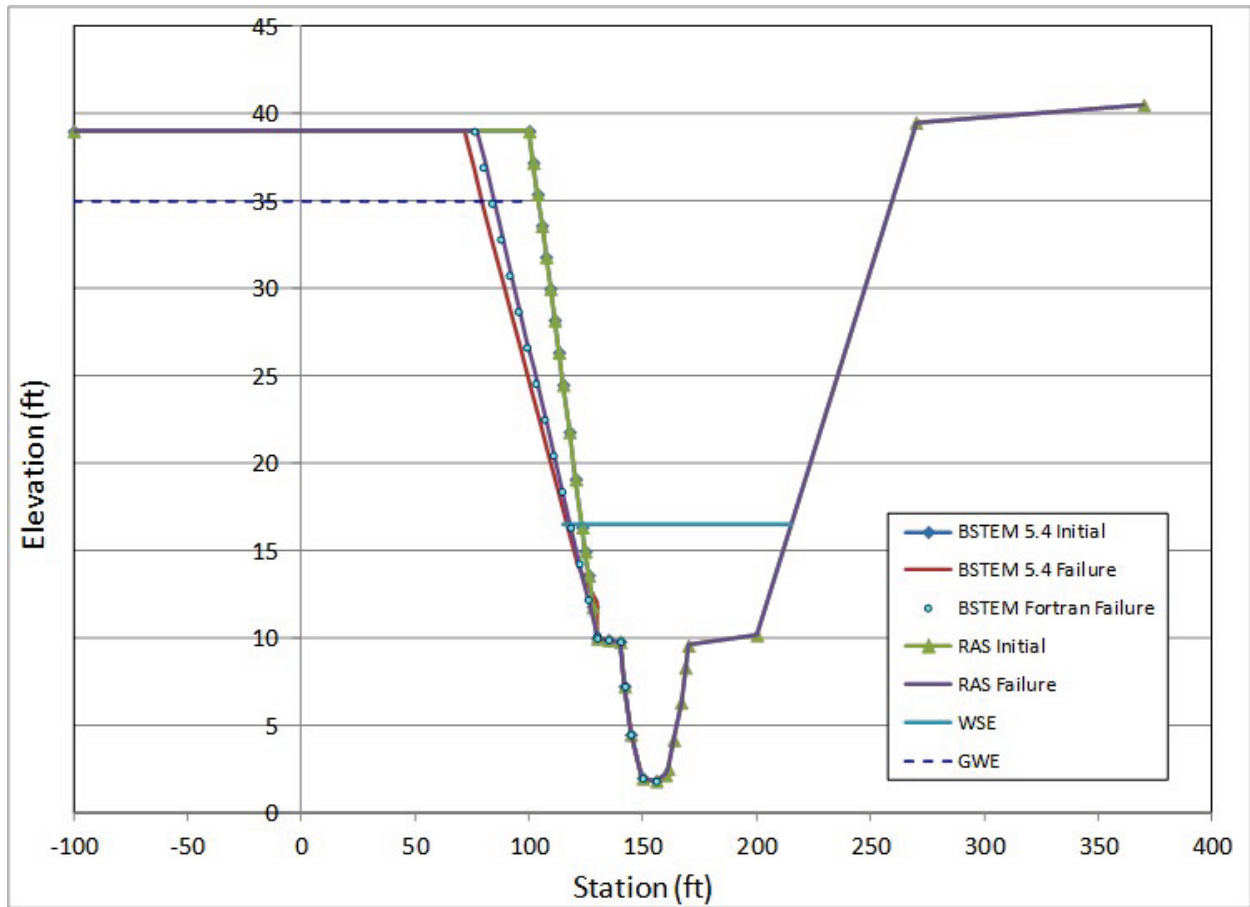


Figure 48. Output from a validation test of the HEC-RAS implementation of the bank failure capabilities and the standalone models.

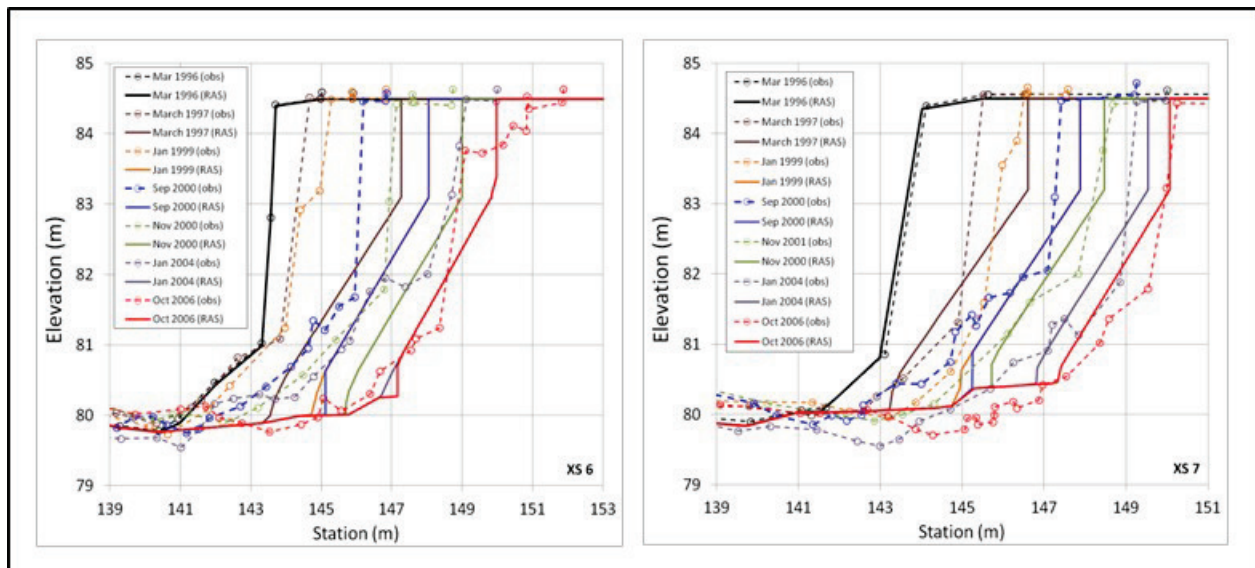


Figure 49. Select Goodwin Creek repeated right bank surveys at the two central cross sections with HEC-RAS/BSTEM cross section migration from Gibson (2015).

Model processes from simple to complex. Add complexity one step at a time. A stepwise modeling process, that adds complexity incrementally, carefully calibrating and evaluating results of each modeling step, will produce more accurate models and sane modelers.

Create an HEC-RAS/BSTEM model in the following incremental steps, carefully completing, evaluating, and calibrating each step before adding the complexity of the next step.

1. **Calibrate Hydraulics:** Create the geometry and calibrate model hydraulics in the steady flow module over the range of expected flows.
2. **Model/Calibrate Sediment Transport:** Isolate the sediment transport mechanics by carefully modeling bed sediment without bank processes first. Build a robust (Thomas, 2007; Gee, 1982) calibrated model, or at least, evaluate results to understand the sensitive parameters.
3. **Model/Calibrate Bank Erosion and Bank Failure:** By setting the cross sections as **Pass-Through Nodes** (under the **Options** menu in the **Sediment Data Editor**), users can isolate bank processes and refine bank methods and parameters without the complexity bed process feedbacks.
4. **Integrate Bank Erosion and Failure plus Mobile Bed Sediment Transport Model:** After the hydraulics are calibrated and the bed and bank sediment models have been refined independently, then combine all the components, and calibrate the coupled model to bed and bank change.

UM.7.2 Selecting a Toe

The USDA-ARS BSTEM model is very sensitive to the toe node selected. Tips for selecting the toe include:

1. Make the **BSTEM Toe Station** the same as the **Movable Bed Limit (Left Station and Right Station in Initial Conditions and Transport Parameters in the Sediment Data Editor)**. While there is a tool to set the **Toe Stations** to the **Movable Bed Limits**, it is often better to go the other way, selecting a toe and then setting the **Movable Bed Limit** station equal to the **Toe Station**.
2. HEC-RAS distorts cross sections vertically in the cross section display of the **Geometry Editor**. This makes them easier to visualize, but can make it difficult to select a toe. When selecting toe stations, change the aspect ratio of the cross section plotter. Adjust the cross section view window to a short-vertical, maximum-horizontal configuration and zoom in along the horizontal axis until one foot or meter of station spacing is equal to one foot or meter or elevation spacing (e.g., a 1:1 H:V ratio; Figure 50). This adjustment will make it easier to pick an actual toe from an undistorted cross section plot.

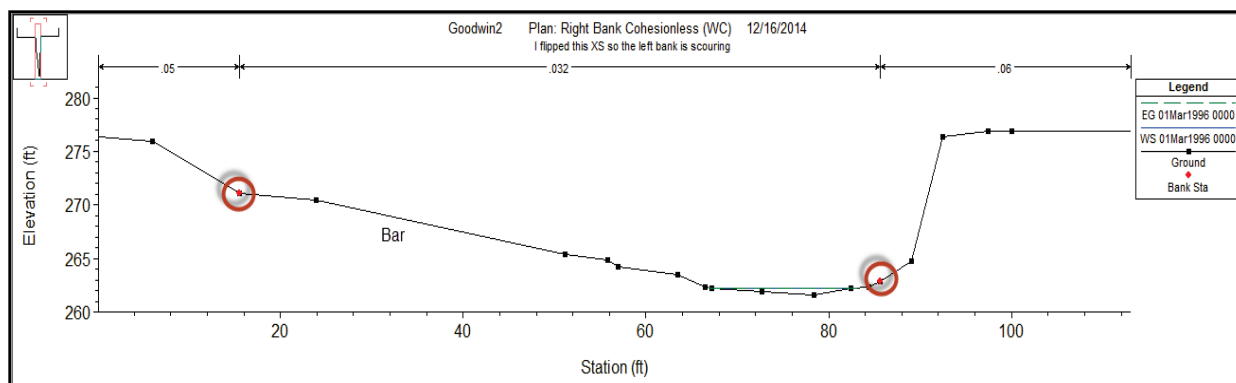


Figure 50. Cross section viewer adjusted to approximately a 1:1 aspect ratio to help select the toe station.

UM.7.3 Monotonic Bank Geometry

HEC-RAS allows complex cross sections. USDA-ARS BSTEM idealizes cross sections in a couple of important ways. HEC added logic to adapt BSTEM to complex cross sections, but some cross sections shapes still tend to be unstable. In particular, avoid "bank depressions" (Figure 51) if possible. Cross section node elevations should increase from the toe to the edge of the bank.

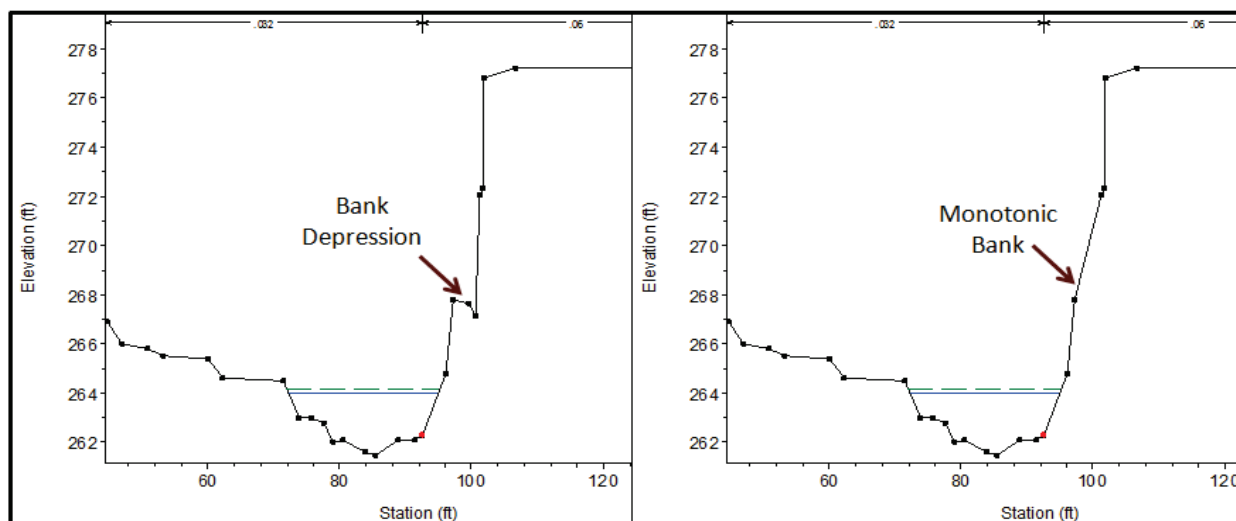


Figure 51. Avoid bank depressions (left) where possible, particularly with soil layers. Monotonic banks (cross section nodes that increase from the toe out to the bank edge) are more stable.

The model can become unstable when a soil layer boundary crosses the cross section more than once. Therefore, if the cross section includes an important bank depression, make sure that the soil layer does not pass through it.

UM.7.4 Floodplain Geometry

The portion of the cross section outside the **Edge of Bank Station** must conform to three conventions to provide optimal results:

1. The floodplain must be wide enough to include the maximum failure plane angle. For long term simulations this includes the maximum failure plane from the maximum scour location. As a rule of thumb, include a floodplain wide enough to encompass at least a ten degree angle from the toe station.
2. The floodplain (or Top of Bank, Figure 27) needs intermediate station-elevation points between the edge of the bank and the end of the cross section (Figure 52) for BSTEM to compute failure planes effectively.

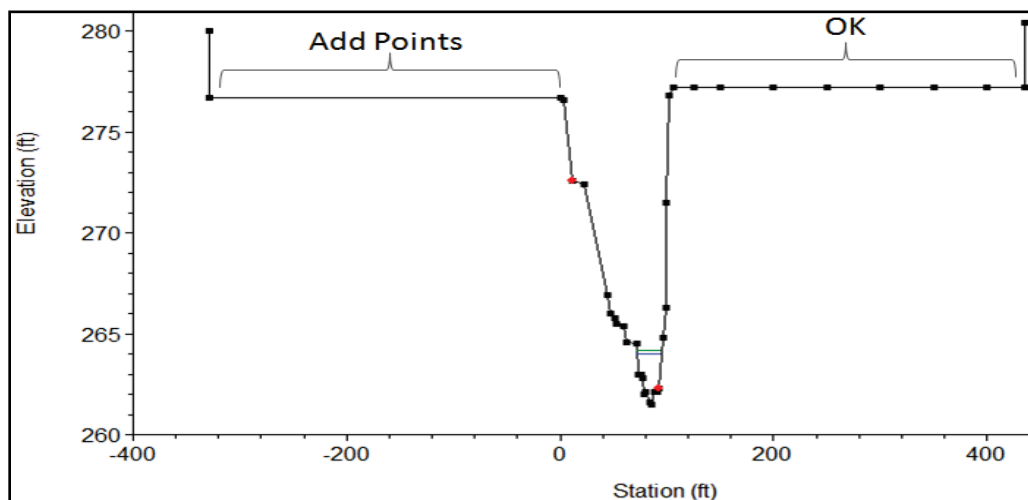


Figure 52. BSTEM requires cross section station-elevation points between the Bank Edge Station and the end of the cross section.

3. If the floodplain is irregular (Figure 39) it should not intersect with a layer more than once. If the cross section includes multiple soil layers, the top layer should include all of the cross section nodes outside of the bank edge station.
4. HEC-RAS should be able to handle wet depressions and ineffective flow areas outside the bank edge, but the more floodplain complexity in a cross section the more likely that the failure plane algorithm will converge on a false maximum or that the cross section update will encounter a problem. Avoid incidental cross section complexity, particularly in the overbank.

UM.7.5 Too Much Toe Scour

Most HEC-RAS/BSTEM model failures come from having too much toe scour. Since soil erodibility data can vary by orders of magnitude, even in the same site, selecting high cohesive erodibility will compute excessive scour. Cohesionless methods (Figure 53), that compute toe scour with transport equations almost always over predict scour, sometimes dramatically.

UM.7.6 Common Runtime Error Messages

The **unrealistic vertical adjustment** error (Figure 54) is the most common sediment error in general and HEC-RAS/BSTEM in particular. This error indicates that HEC-RAS computed very large bed changes at the indicated cross section in the last timestep before the program stopped.

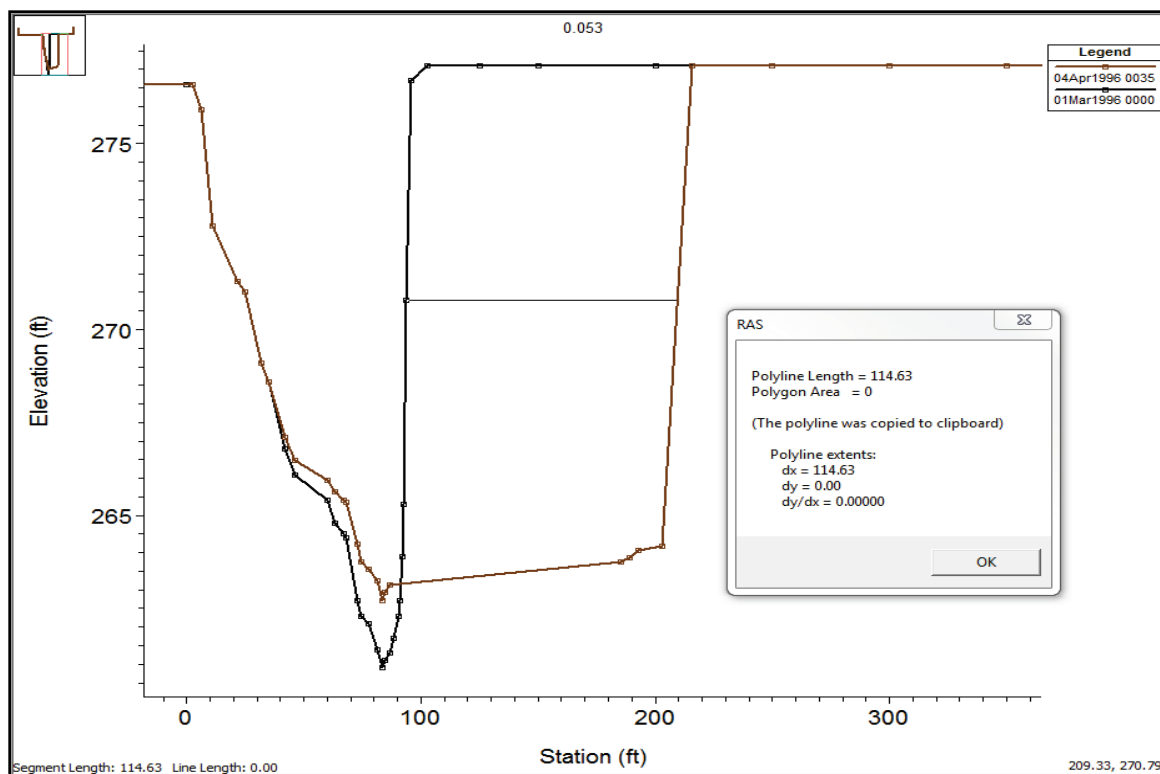


Figure 53. In this model, the cohesionless transport methods computed more than 100 feet of bank scour in just over a month, which is order of magnitude faster than the actual bank recession rate.

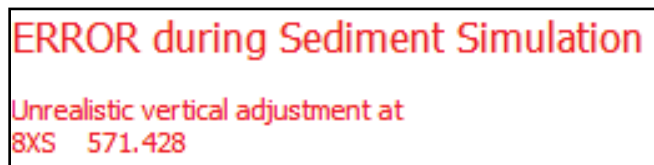


Figure 54. The Unrealistic Vertical Adjustment Error.

This error is often resolved by reducing the computation increment. However, sometimes more systemic model or data problems make the error persist at very small computational increments. The most common causes include:

1. Excessive toe scour: The most common cause of model failure is excessive toe scour (Section UM.7.5). Lower the erodibility substantially or turn off the cohesionless transport methods (go to the **BSTEM Options Editor** under the **Options** menu in the **Sediment Data Editor**) to stabilize the model.
2. Bed material does not match transport function: If the bed material is too fine for the transport function, or if the transport function over predicts transport in the reach, the mismatch can lead to large, rapid bed changes, destabilizing the model. A common error involves assigning fine bank material gradations to the bed.
3. Equilibrium Load: If the equilibrium load boundary condition is used with bed gradations that include non-trivial amounts of silt or clay, this boundary condition can compute enormous fine-grained sediment loads at the boundary. Small decreases in transport

downstream can cause large bed changes. User-defined rating curves are almost always better sediment boundary condition options, even if they are speculative.

UM.7.7 Unusual Cross Section Shape

Sometimes active cross sections can produce strange shapes, like the example shown in Figure 55. First, make sure the toe station and the movable bed limits are set to the same station. Second, the USDA-ARS BSTEM features often work best if HEC-RAS allows deposition outside the movable bed limits. From the **Sediment Data Editor**, from the **Options** menu, select **Bed Change Options**. Then, under **Deposition**, select **Allow Deposition Outside of the Movable Bed Limits**. This will constrain erosion to the movable bed limits (which will migrate with the toe if they have the same starting station) but will deposit at any wetted node in the cross section. The model in Figure 55 was re-run in Figure 56 with this option selected and produced more realistic results.

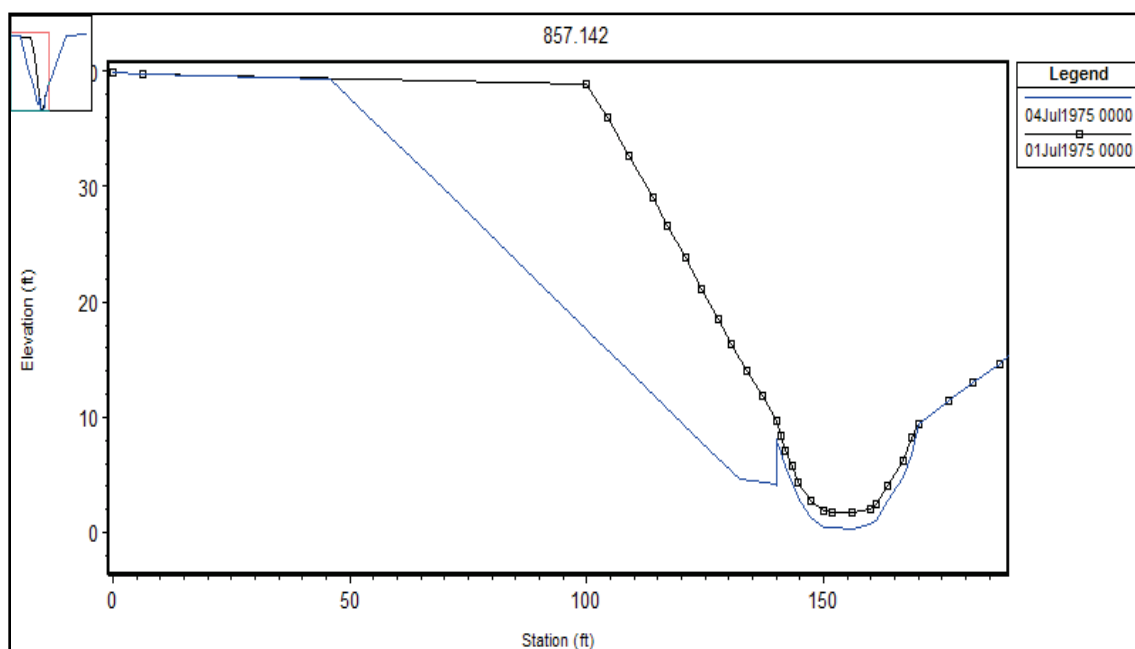


Figure 55. Strange cross section shape caused by deposition inside the movable bed limits, but not outside.

UM.7.8 Groundwater Table

Results can be very sensitive to groundwater. Two particular groundwater errors that can create model problems:

1. Never specify a starting or static groundwater table that is higher than the bank edge.
2. Groundwater elevations far below the channel water surface elevation will keep the bank from failing. The USDA-ARS BSTEM applies a hydrostatic assumption, computing suction according to a hydrostatic gradient from the groundwater elevation. Therefore, in ephemeral streams or situations where the groundwater table is unknown, estimate the groundwater elevation or put it at an average surface water elevation at which banks should fail.

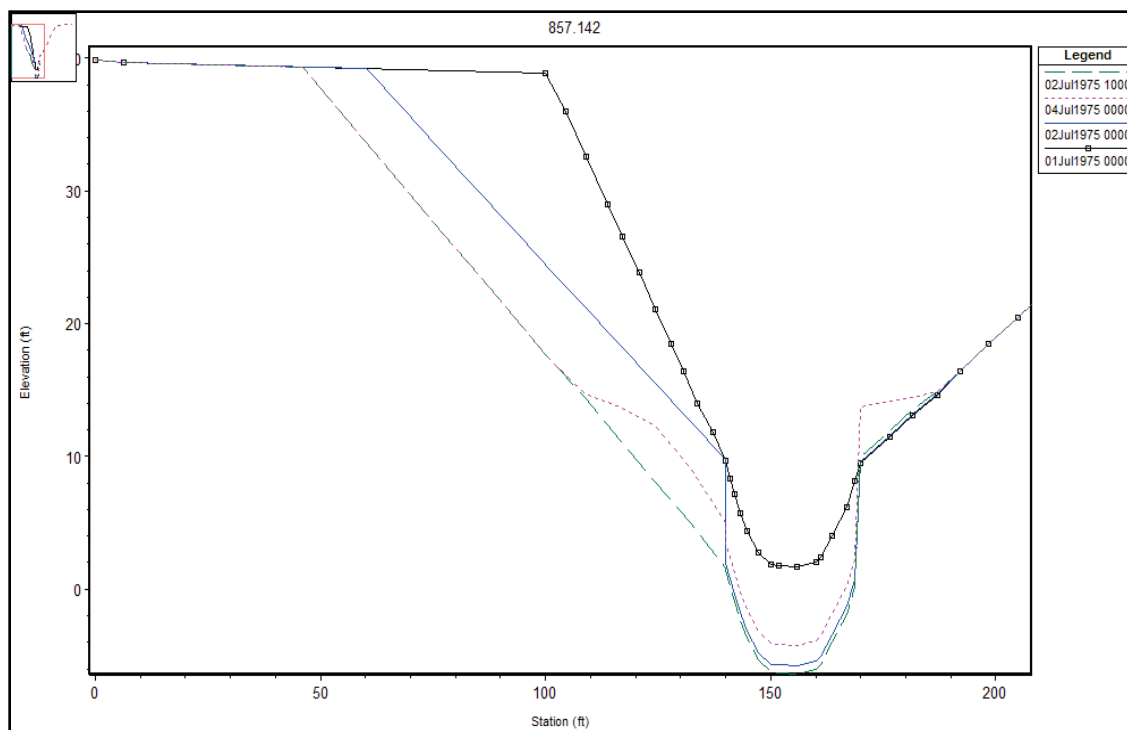


Figure 56. The same simulation as Figure 55, but allowing for deposition in the overbanks.

UM.7.9 Scour Outside of a Bend

In natural systems, banks are usually most active on the outside of a bend or meander. HEC-RAS is a one-dimensional model and does not simulate the multi-dimensional forces that cause this preferential erosion. Banks migrate more on the outside of bends because multi-dimensional effects produce higher shears there. Because HEC-RAS uses an excess shear equation to compute scour, users can simulate preferential bank scour by decreasing the critical shear at bend cross sections. This will approximate the physical process, increasing the $(\tau - \tau_c)$ shear difference by decreasing the critical shear instead of increasing the shear.

UM.8 Acknowledgements

The integration of the USDA-ARS Bank Failure and Toe Erosion Methods (BSTEM) in HEC-RAS has been a significant effort with multiple funding partners including:

- Regional Sediment Management Program (USACE)
- Missouri River Recovery Project (USACE)
- The Australian Rivers Institute
- Flood and Coastal Storm Damage Reduction R&D Program (USACE)

HEC has also collaborated with and received code and/or technical guidance from:

- Andrew Simon PhD and Natasha Bankhead PhD (Cardno Entrix)
- Eddy Langendoen PhD and the USDA-ARS
- U.S. Bureau of Reclamation

The integration of HEC-RAS and BSTEM has been a substantial undertaking including multiple contributors in the USACE, the private sector, other Federal agencies, and even international interests. Andrew Simon (PhD - Cardno ENTRIX, formerly of USDA-ARS) partnered with HEC to initiate, envision and facilitate the integration. Eddy Langendoen (PhD - USDA-ARS) has provided essential technical support and advice throughout the process. The integration utilized code developed by Rob Thomas (PhD - University of Hull, formerly of University of Tennessee) and Yong Lai (PhD - USBR), funded by the Bureau of Reclamation and the Taiwanese Water Resources Agency, with input from Yavuz Ozeren (PhD - University of Mississippi). John Shelly (PhD - NWK) and Paul Boyd (PhD - NWO) provided District guidance and feedback on the development. Stanford Gibson (PhD - HEC) and Steve Piper (RMA) worked on the integrated HEC-RAS code. Funding for the development, troubleshooting, and documentation of the integrated HEC-RAS/BSTEM product has come from multiple sources including two USACE R&D Programs (Regional Sediment Management and Flood & Coastal Storm Damage Reduction), the Australia Rivers Institute, and the Missouri River Recovery Program.

UM.9 Scour Units

The cohesive model used in the bed model is different than that used in the bank model. The bed model removes sediment by mass. Mass is removed per area, per time in response to a force (e.g., N/m²-hr/Pa which translates to the slope of the relationship between mass removed per area per time and the force, which is one/time). In the bank model a volume is removed in response to a force, so the units are volume/force-time (e.g., M³/Pa-hr).

This difference is because bulk mass is removed from the bed and applied uniformly over the bed. The bank model shifts each node laterally, independently. Therefore, a "volume" is translated into a lateral shift, per node.

The following table provides conversion factors to move between SI and U.S. customary units.

Table 4. Conversion Factors.

From	Multiply by	To
m ³ /N/s	0.42	1/hr
Pa	0.0208	psf
m ³ /N-s	6365.9	ft ³ /lbf-s
1/hr	2.39	m ³ /N/s
psf	47.9	Pa
ft ³ /lbf-s	0.000157	m ³ /N-s

UM.10 SI Table

Table 5. Default materials and material parameters.

Default Material Type	Saturated Unit Weight (kN/m ³)	Friction Angle (ϕ)	Cohesion (kPa)	ϕ^b	Critical Shear (Pa)	Erodibility (m ³ /N-s)
Boulders	20.0	42.0	0	15	498	4.48E-09
Cobbles	20.0	42.0	0	15	124	9.00E-09
Gravel	20.0	36.0	0	15	11	3.02E-08
Coarse Angular Sand	18.5	32.3	0.4	15	0.506	1.41E-07
Course Round Sand	18.5	28.3	0.4	15	0.506	1.41E-07
Fine Angular Sand	18.5	32.3	0.4	15	0.128	1.41E-07
Fine Round Sand	18.5	28.3	0.4	15	0.128	1.41E-07
Erodible Silt	18.0	26.6	4.3	15	0.1	3.16E-07
Moderate Silt	18.0	26.6	4.3	15	5	4.50E-08
Resistant Silt	18.0	26.6	4.3	15	50	1.40E-08
Erodible Soft Clay	17.7	26.4	8.2	15	0.1	3.16E-07
Moderate Soft Clay	17.7	26.4	8.2	15	5	4.50E-08
Resistant Soft Clay	17.7	26.4	8.2	15	50	3.16E-07
Erodible Stiff Clay	17.7	21.1	12.6	15	699.1	3.16E-07
Moderate Stiff Clay	17.7	21.1	12.6	15	5	4.50E-08
Resistant Stiff Clay	17.7	21.1	12.6	15	50	3.16E-07

UM.11 References

Bishop, 1995

Bishop, A. W. (1955). *The use of the slip circle in the stability analysis of slopes*. Géotechnique, 5:7-17.

Borrowman, 2006

Borrowman, T. D., Smith, E. R., Gailani, J. Z., and Caviness, L. (2006). *Erodibility Study of Passaic River Sediments Using USACE Sedflume*. Engineer Research and Development Center Paper ERDC-TR-06-7. Engineer Research and Development Center Environmental Lab, Vicksburg, MS.

Casagli, 1999

Casagli, N., Rinaldi, M., Gargini, A., and Curini, A. (1999). *Pore water pressure and streambank stability: results from a monitoring site on the Sieve River, Italy*. Earth Surface Processes and Landforms, 24(12): 1095-1114.

Engelund, 1967

Engelund, F., and Hansen, E. (1967). *A monograph on sediment transport in alluvial streams*. Technical University of Denmark Østervoldgade 10, Copenhagen K.

Fredlund, 1996

Fredlund, D. G., Xing, A., Fredlund, M. D., and Barbour, S. L. (1996). *The relationship of the unsaturated soil shear to the soil-water characteristic curve*. Canadian Geotechnical Journal, 33(3), 440-448.

Gee, 1982

Gee, D. Michael (1982). *Guidelines for the Calibration and Application of the Computer Model HEC-6*, Training Document No. 13, USACE, Hydrologic Engineering Center, Davis, CA; 13 pages.

Gibson, 2006

Gibson, S., Brunner, G., Piper, S., and Jensen, M. (2006). *Sediment Transport Computations in HEC-RAS*. Eighth Federal Interagency Sedimentation Conference (8thFISC), Reno, NV, 57-64.

Gibson, 2015

Gibson, S., Simon, A., Langendoen, E., Bankhead, N., Shelley, J. (2015). *A Physically-Based Channel-Modeling Framework Integrating HEC-RAS Sediment Transport Capabilities and the USDA-ARS Bank-Stability and Toe-Erosion Model (BSTEM)*, SEDHYD Federal interagency conference.

Hanson, 2001

Hanson, G. J., and Simon, A. (2001). *Erodibility of cohesive streambeds in the loess area of the Midwestern USA*. Hydrological processes, 15(1): 23-38.

HEC, 2016a

U.S. Army Corps of Engineers, Hydrologic Engineering Center (2016). *HEC-RAS River Analysis System, User's Manual, Version 5.0*, CPD-68. Hydrologic Engineering Center, Davis, CA.

HEC, 2016b

U.S. Army Corps of Engineers, Hydrologic Engineering Center (2016). *HEC-RAS River Analysis System, User's Manual, Version 5.0*, CPD-68. Hydrologic Engineering Center, Davis, CA.

Kean, 2001

Kean, J. W. and Smith, J.D. (2001). *Computation of sediment erosion from the base of cut banks in river bends*. Seventh Federal Interagency Sedimentation Conference (7thFISC), Reno, NV, V-31.

Komar, 1987

Komar, P. D. (1987). *Selective gravel entrainment and the empirical evaluation of flow competence*. Sedimentology, 34(6): 1165-1176.

Lai, 2015

Lai, Y. G., Thomas, R. E., Ozeren, Y., Simon, A., Greimann, B. P., and Wu, K. (2015). *Modeling of multilayer cohesive bank erosion with a coupled bank stability and mobile-bed model*. Geomorphology, 243: 116-129. doi: 10.1016/j.geomorph.2014.07.017.

Labuz, 2012

Labuz, J. F., & Zang, A. (2012). *Mohr–Coulomb Failure Criterion*. The ISRM Suggested Methods for Rock Characterization, Testing and Monitoring: 2007-2014 (pp. 227-231). Springer International Publishing.

Lambe, 1969

Lambe, T. W., and Whitman, R. V. (1969). *Soil mechanics*. New York, NY, Wiley, 553 p.

Langendoen, 2008

Langendoen, E.J. and Simon, A. (2008). *Modeling the evolution of incised streams, II: Streambank erosion*. Journal of Hydraulic Engineering, 134(7): 905-915.

Millar, 1993

Millar, R. G., and Quick, M. C. (1993). *Effect of bank stability on geometry of gravel rivers*. Journal of Hydraulic Engineering, 119(12): 1343-1363.

Morgenstern, 1965

Morgenstern, N.R. and Price, V.E. (1965). *The analysis of the stability of general slip surfaces*, Géotechnique, 15(1): 79-83.

Parker, 1990

Parker, G. (1990). *Surface-based bedload transport relation for gravel rivers*. Journal of hydraulic research, 28(4), 417-436.

Shelley, 2015

Shelley, J., Gibson, S., and Williams, A. (2015). *Unsteady Flow and Sediment Modeling in a Large Reservoir Using HEC-RAS 5.0*, Federal Interagency Sediment Conference.

Simon, 2010

Simon A., Thomas, R., and Klimetz, L. (2010). *Comparison and Experiences with Field Techniques to Measure Critical Shear Stress and Erodibility of Cohesive Deposits*, 2nd Joint Federal Interagency Conference, Las Vegas, NV, June 27 - July 1, 2010.

Simon, 2012

Simon, A., Ozeren, Y., and Thomas, R. E. (2012). *Comparison of the Bank-Stability Sub Model with in the Visual Basic and FORTRAN Versions of (BSTEM)*, 18p.

Simon, 2000

Simon, A., Curini, A., Darby, S.E., and Langendoen, E.J. (2000). *Bank and near-bank processes in an incised channel*, Geomorphology, 35: 193-217.

Simon, 2008a

Simon, A., Derrick, D., Alonso, C., and Pollen-Bankhead, N. (2008). *Application of a deterministic bank-stability model to design a reach-scale restoration project*. In World Environmental and Water Resources Congress 2008: Ahupua'A (pp. 1-9).

Simon, 2008b

Simon, A., Derrick, D., Alonso, C.V., and Bankhead, N.L. (2008). *Application of a deterministic bank-stability model to design a reach-scale restoration project*. Proc. ASCE-EWRI, World Environmental Water Resources Congress, Honolulu, Hawaii, 10 p. (on CD).

Simon, 2011

Simon, A., Pollen-Bankhead, N., and Thomas, R.E. (2011). *Development and application of a deterministic bank stability and toe-erosion model for stream restoration*. Stream Restoration in Dynamic Fluvial Systems: Scientific Approaches, Analyses, and Tools. A. Simon, S.J. Bennett, and J.M. Castro (Eds.), Geophysical Monograph Series, 194, 500 p. ISBN 978-0-87590-483-2, Washington, DC.

Teukolsky, 2007

Teukolsky, S.A., Vetterling, W.T., and Flannery, B.P. (2007). *Numerical Recipes: The Art of Scientific Computing*, Cambridge University Press; 3 edition, 1256 p.

Thomas, 2007

Thomas, William, A. and Chang, H. (2007). *Computational Modeling of Sedimentation Process, Sediment Engineering: Processes, Measurements, Modeling, and Practice – ASCE Manuals and Reports on Engineering Practice 110*, ed. M.H. Garcia, 649-681.

Thorne, 1981a

Thorne, C. R., & Tovey, N. K. (1981). *Stability of composite river banks*. Earth Surface Processes and Landforms, 6(5): 469-484.

Thorne, 1981b

Thorne, C.R. (1981). *Field measurements of rates of bank erosion and bank material strength. Erosion and Sediment Transport Measurement*. Proceedings of the Florence Symposium, IAHS Publication 133, 503-512.

Wilcock, 2003

Wilcock, P. R., & Crowe, J. C. (2003). *Surface-based transport model for mixed-size sediment*. Journal of Hydraulic Engineering, 129(2): 120-128.

Yang, 1973

Yang, C. T. (1973). *Incipient motion and sediment transport*. Journal of the hydraulics division, 99(10): 1679-1704.

